Source: STANDARD HANDBOOK OF ELECTRONIC ENGINEERING

CHAPTER 8.5
MICROSENSORS AND MICROACTUATORS

Wen H. Ko, C. C. Liu, M. Mehregany

INTRODUCTION

The term *microelectromechanical systems* (MEMS) was coined around 1987. Besides microfabricated sensors and actuators, the field includes micromechanical components and microassembled systems. The field of microtransducers traditionally has been application driven and technology limited, and has emerged as an interdisciplinary field that involves many areas of science and engineering. MEMS is expected to follow a similar trend.

Microelectromechanical devices and systems are inherently smaller, lighter, faster, and usually more precise than their macroscopic counterparts. However, development of micromechanical systems requires appropriate fabrication technologies that enable the definition of small geometries, precise dimensional control, design flexibility, interfacing with control electronics, repeatability, reliability and high yield, and low cost per device. IC fabrication technology meets all of the above criteria and has been the primary enabling technology for the development of micromechanical systems. Microfabrication provides a powerful tool for batch processing and miniaturization of mechanical systems into a dimensional domain not accessible by conventional (machining) techniques. It provides an opportunity for integration of mechanical systems with electronics to develop high-performance closed-loop functional MEMS. In its most general form, MEMS would consist of mechanical microstructures, microsensors, microactuators, and information processing electronics integrated in the same package. This chapter will emphasize microsensors and microactuators.

MICROMACHINING TECHNOLOGY

Micromachining is a key fabrication technology for solid-state sensors and actuators, as well as MEMS. There are two classifications of micromachining, bulk and surface, both of which are based on silicon IC technology. In surface micromachining, the shaping is done only on one or both surfaces of a substrate material. Bulk and surface micromachining include techniques for selective etching, deposition, bonding, and packaging. The deposition technology is the same as that used in IC fabrication; the packaging is a developing technology that differs with each situation. Therefore, the major discussion on micromachining usually concentrates on etching and bonding and other special processes.

Downloaded from Digital Engineering Library @ McGraw-Hill (www.digitalengineeringlibrary.com)
Copyright © 2004 The McGraw-Hill Companies. All rights reserved.
Any use is subject to the Terms of Use as given at the website.

MICROSENSORS AND MICROACTUATORS

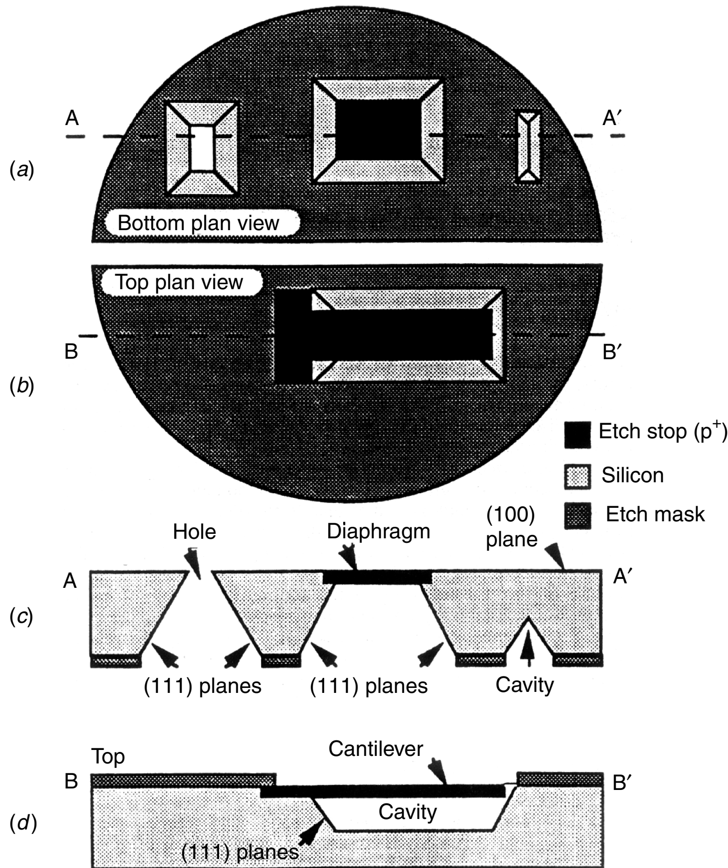

FIGURE 8.5.1 The basic concepts of bulk micromachining. (*a*) The bottom plan view of an anisotropic etched wafer showing the fabrication of cavities, diaphragms, and holes. (*b*) The top plan view of an anisotropically etched wafer showing the fabrication of a cantilever beam using etch stop layers. (*c*) The cross section, A-A′, showing the hole, diaphragm, and cavity of (*a*). (*d*) The cross section, B-B′, showing the cantilever beam of (*b*).

Bulk Micromachining

There are two techniques that make micromachining of silicon viable: (1) anisotropic etchants of silicon that preferentially etch single crystal silicon along selected crystal planes, and (2) etch masks and etch-stop techniques used in conjunction with silicon anisotropic etchants to selectively prevent regions of silicon from being etched. By appropriately combining etch masks and etch-stop patterns with anisotropic etchants, three-dimensional microstructures in a silicon substrate can be fabricated with high accuracy. Figure 8.5.1 shows two basic concepts of bulk micromachining.

Surface Micromachining

Surface micromachining relies on encasing the structural parts of the device in layers of a sacrificial material during the fabrication process. The sacrificial material (also called spacer material) is then dissolved away in

Downloaded from Digital Engineering Library @ McGraw-Hill (www.digitalengineeringlibrary.com)
Copyright © 2004 The McGraw-Hill Companies. All rights reserved.
Any use is subject to the Terms of Use as given at the website.

MICROSENSORS AND MICROACTUATORS

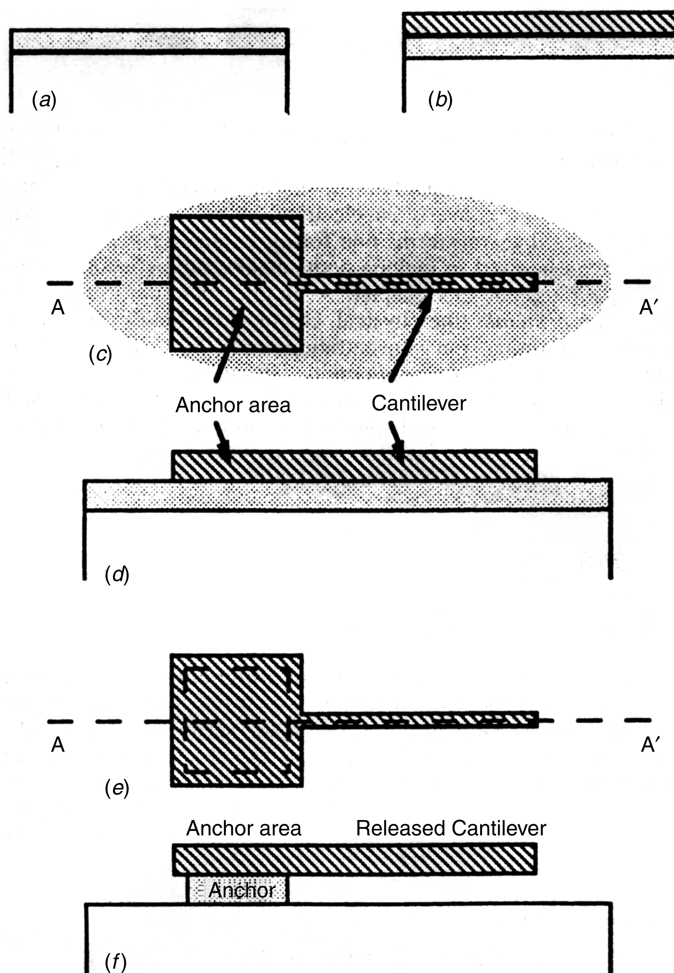

FIGURE 8.5.2 Schematics demonstrating surface micromachining in its simplest form: (*a*) cross-sectional view after the sacrificial layer is deposited; (*b*) cross-sectional view after the structural layer is deposited; (*c*) top plan view after patterning of the structural layer; (*d*) cross section AA′ of (*c*); (*e*) top plan view after release; and (*f*) cross section AA′ of (*e*).

a chemical etchant that does not attack the structural parts. The final stage of dissolving the sacrificial layer is called "release." In other words, there are two primary components in a surface micromachining process: (1) *structural* layers of which the final microstructures are made and (2) *sacrificial* layers that separate the structural layers and are dissolved in the final stage of device fabrication. The basic concepts and principles of surface micromachining are given below.

Figure 8.5.2 describes one of the simplest forms of surface micromachining in which only two film depositions (i.e., one sacrificial and one structural) followed by one patterning step (i.e., for the structural layer) are needed for device fabrication. The sacrificial layer is deposited first, followed by the deposition of the structural layer. The structural layer is then patterned, forming the cantilever and the anchor region in our example. At this point, the release step is performed, creating a cantilever suspended over the substrate at a height that is flush with the surface of the silicon.

Downloaded from Digital Engineering Library @ McGraw-Hill (www.digitalengineeringlibrary.com)
Copyright © 2004 The McGraw-Hill Companies. All rights reserved.
Any use is subject to the Terms of Use as given at the website.

Bonding

In micromachining, bonding techniques are used to assemble individually micromachined parts to form a complete structure. Usually entire wafers or individual dies are bonded together. Wafer bonding allows the fabrication of three-dimensional structures that are thicker than a single wafer. This is important for micro-pumps and microvalves where more than one cavity is needed in the thickness direction. Several processes have been developed for bonding silicon wafers. A review of bonding techniques is given by Ko, et al.[4] and Tong.[5] Fusion bonding was developed to bond silicon to silicon and to many other materials for MEMS (Kovacs 1998, Wolf 1986).

Dry Etch and Deep Reactive Ion Etch

Dry etch processes replace wet etches for precise pattern transfer and simple operation. There are many types of dry etch techniques developed for IC processes including gas discharge methods and ion beam methods. They are used in micromachining. The deep reactive ion etch can be used to fabricate structures with great depth and controlled wall profile. It is an important process for etching devices with high aspect ratio (ratio of height to width).

LIGA and High Aspect Ratio Processes

LIGA (a German acronym for Lithographie, Galvanoforming, Abformung) process uses lithography of thick photo resist and x-ray exposure to produce a desired structure, then uses metal electroplating to generate a complementary metal mold, and microinjection molding to fabricate multiple replicas of the original. This process is used to fabricate high aspect ratio structures that are difficult to make with conventional MEMS process (Ref. 7). A Synchrotron accelerator provides x-ray exposure. Other high-aspect ratio lithography employs ultraviolet and other techniques (Ref. 8).

Packaging

Hermetic seal, lapping, polishing, and assembly techniques for microsystems as well as protection package processes were developed to bring MEMS from laboratory to market place. However, the technology is developing and each technique is applicable to a small group of applications. There are no universal package methods available and this is a field of intense research.

Micromachining of Other Materials

Micromachining of compound semiconductors, quartz, glass, ceramic, and polymeric materials for optical communication, chemical, biological, and medical applications is possible. Large-scale manufacturing methods for microdevices including injection molding, precision plating, and microassembly are anticipated.

DEFINITIONS

As in the case of other instrumentation systems, MEMS can be deemed to consist of an input block (sensor), output block (actuator), and signal processing block (electronics). A *sensor* is a device that provides a usable electrical output signal in response to a specified measurand. An *actuator*, the reverse of a sensor, is a device that converts an electrical signal to an action, while a *transducer* can be considered as the device that transforms one form of signal or energy into another form. Therefore, the term transducer can be used to include both sensors and actuators. These definitions, though not universal, are used throughout this chapter. A number of criteria can be used to classify sensors, including *transduction principle* (the physical, chemical, or biological effects), *measurands* (e.g., pressure, acceleration, gas concentration, ion concentration), *fabrication*

Downloaded from Digital Engineering Library @ McGraw-Hill (www.digitalengineeringlibrary.com)
Copyright © 2004 The McGraw-Hill Companies. All rights reserved.
Any use is subject to the Terms of Use as given at the website.

technology and materials (e.g., thin film, semiconductors, ceramics) *applications* (e.g., automotive, medical, aerospace), and *cost and performance*. In most of the literature, a combination of principle, measurand, and application is used to define sensors and actuators. This chapter will follow the popular approach of classifying sensors into three major groups: *physical, chemical*, and *biomedical*.

PHYSICAL MICROSENSORS

Integrated, Intelligent (Smart) Sensors

When a microsensor is integrated with signal processing circuits in a single package, it is referred to as an integrated sensor. A monolithic integrated sensor has the signal processing circuit fabricated on the same chip as the sensor, while a hybrid integrated sensor has the signal processing circuit on the same hybrid substrate as the sensor chip. The packaged sensor not only transduces the measurand into electrical signals, but also may have other signal processing and decision-making capabilities. Thus, the term *intelligent sensors* was coined.[9] In trade journals and popular news articles they are also called smart sensors. Integrated sensors with specific types of on-chip electronic circuits may have the following advantages:

Better signal-to-noise ratio.

Improved characteristics. Signal processing can provide: (a) on-chip feedback system or look-up tables to improve the output linearity, (b) compensation circuits to reduce cross-sensitivity to temperature, strain, or other known interfering effects, (c) on-chip accurate current and voltage sources and associated circuits to provide automatic and periodic self-checking and calibration, and (d) feedback and other circuits to improve or compensate for the frequency response of the sensor.

Signal conditioning and formatting. Signal conditioning can be performed by integrated circuits prior to the output, such as (a) A-to-D conversion, (b) impedance matching, (c) output formatting to a standard, and (d) signal averaging.

Improved signals representing the measurands. Decision-making and computing circuits as well as memory devices may be used with redundant sensors to exclude noisy or failed sensors from the array of devices, thus improving the signal beyond a single sensor's capability. Multiple sensors, each with poor selectivity to a family of measurands, can be used with pattern recognition circuits to obtain accurate signals for each of the measurands. Neural networks may be used to train the sensors to recognize the desired measurands among several interfering effects. Many of the signal processing techniques used so successfully in communications and defense applications may be incorporated with the sensors to improve the quality of the sensor output beyond the individual device's capability. A brief summary of commonly used physical sensors follows.

Thermal Sensors

The best-known thermal sensors are thermistors and thermocouples for measuring the temperature of the environment. Thermistors and resistive temperature detectors (RTDs) are based on the change of mobility and carrier density with temperature. These changes are represented by temperature coefficients that may be constants or nonlinear functions of temperature. The resistance of a thermistor is an exponential function of the temperature. Linearization networks may be used to make the output a linear function of the temperature over a specific range, with some sacrifice in sensitivity.

The thermocouple is based on the Seebeck effect, one of the three thermoelectric effects (Seebeck, Peltier, and Thompson effects). Two different materials (usually metals) are joined at one point to form a thermocouple. Various metal wires can be used as thermocouples for different temperature ranges and sensitivity. Common wire materials are: iron/constantan, chromel/constantan, and platinum/platinum +10 percent rhodium. Semiconductors, including silicon, may also be used with a metal to form a microthermocouple by micromachining techniques. Hundreds of these microthermocouples may be connected in series on a silicon

Downloaded from Digital Engineering Library @ McGraw-Hill (www.digitalengineeringlibrary.com)
Copyright © 2004 The McGraw-Hill Companies. All rights reserved.
Any use is subject to the Terms of Use as given at the website.

chip to form a thermopile microsensor that is hundreds of times more sensitive than a single thermocouple. These microthermosensors are sensitive enough to measure the temperature rise in millidegree centigrade as a result of incident infrared radiation (IR), making them useful as IR imaging sensors and remote temperature sensors.[10]

If the current through a *p-n* junction is kept constant, the junction voltage is a linear function of temperature. This principle has been used for many commercial temperature sensors. When two bipolar transistors are operated at a constant ratio of emitter current densities, the difference in base emitter voltages is proportional to the absolute temperature. This principle is the basis of many precise commercial temperature sensor ICs.

The mass flow of fluids can be measured by the temperature difference between two sensors, one on the downstream and one on the upstream of a heating (or cooling) source. This is the principle of microanemometers and is also a good example of how the mechanical measurand (flow) is reduced to thermal parameters that are then transduced to electrical signals.

Electrical Sensors

Electrical signals can be picked up by *ideal* ohmic connections without special sensors. However, most connections and electrical probes are not *ideal* and, sometimes, the magnitude of the charge, currentm, and voltage may not be convenient to measure directly. For example, Hall effect sensors are used to measure the current and polarity in motor windings where the current value is very large or a contact is difficult to make. Similarly, electrical sensors may be used to measure very high voltages or very large charges.

The flow of electrical currents occurs through the motion of charge carriers that may be electrons (and holes), ions, and charged defects in materials. These different charge carriers can have very different charge-to-mass ratios and mobilities. When a current has to pass from a material with one type of charge carrier (e.g., electrons) through the interface to another material with a different type of charge carrier (e.g., ions), there are complex reactions occurring at the interface associated with the transfer of charges. The charge carriers in metals are electrons, and in semiconductors may be electrons or holes (the collective behavior of electrons). In electrolytes, the movement of ions carries the current. In dielectrics, it is much more complicated because electrons, ions, charged atom groups, and combinations of these can carry the current. The electrodes that are used to measure electrical parameters in electrolytes or dielectrics are electrical sensors. These electrodes are used in electrochemistry, material science, and biology. The equivalent circuit of such electrodes may include several resistance-capacitance (RC) networks to model the several layers of carriers near the interface. The characterization of the electrode may involve many techniques. A commonly used method is to plot the imaginary part of the impedance versus the real part. In all applications, it is important to know the RC equivalent circuit of the electrodes, the contact potential (work function difference) between the materials in contact, and the thermoelectric effects between the materials in the measurement loop. Using specialized computer programs, the equivalent circuit of the electrode may be found. Noble metal (platinum) wires coated with various materials may be used to measure the potential of the electrolyte, or the ionic concentration of the ions in the electrolyte. These chemical sensors are called *ion selective electrodes* and are used in many chemical and biomedical applications.

Microelectrodes were designed for the measurement of electrical potentials on the surfaces of tissues, cells, and other materials. Vibrating microelectrodes can be used to measure the potential or charge the surface without making direct contact to it.

Mechanical Sensors

There are many mechanical sensors described in the literature and commercially available.[3] Mechanical parameters may be converted to other energy domains and then sensed or measured directly. For direct sensing, the parameters are related to strain or displacement. Silicon, a brittle material, will fail (break) at a maximum strain of about 2 percent. However, below the elastic limit the strain is related to the stress by a nearly constant Young's modulus, which is less than but close to that of steel. The principles commonly used to sense strain are piezoelectricity, piezoresistivity, and capacitive or inductive impedance.

Downloaded from Digital Engineering Library @ McGraw-Hill (www.digitalengineeringlibrary.com)
Copyright © 2004 The McGraw-Hill Companies. All rights reserved.
Any use is subject to the Terms of Use as given at the website.

Piezoelectricity. The piezoelectric effect relates the elastic strain S (or stress T) in one orientation to displacement charge density D (or electric field intensity E) in another orientation that may or may not be the same as the orientation of the strain, through the piezoelectric coefficients. The piezoelectric coefficients are, in general, a $(n \times m)$ matrix, where n is the number of orientations for strain—the mechanical parameter, and m is the number of orientations for D or E—the electrical parameters. The four parameters S, T, D, and E are interrelated by various coefficients or constants. For most applications, simplifying assumptions can be made so that only parallel and perpendicular orientation between the mechanical and electrical parameters are considered. For example, d_{ij} is the strain constant or charge constant of piezoelectricity relating D and T when E is constant, or S and E, when T is constant:

$$D_i = d_{ij}T_j + \epsilon E_i \tag{1}$$

and

$$S_j = YT_j + d_{ji}E_i \tag{2}$$

where ϵ is the dielectric constant or permittivity; and I/Y is the Young's modulus of the material. The coefficient $d_{33} = (\Delta D/\Delta T)_{E=k}$ or $d_{33} = (\Delta S/\Delta E)_{T=k}$, relates D and T or S and T when they are both oriented in the "$z - 3$" direction; thus, they are in parallel. d_{31} relates the electrical parameters D_3 and E_3 to the perpendicular mechanical parameters T_l and S_l.

These coefficients can be used to estimate the characteristics of sensors and actuators. The piezoelectric effect of sensors is used to measure various forms of strain or stress. Examples are microphones for strains generated by acoustic pressure on a diaphragm; ultrasonic sensors for high-frequency strain waves arriving at or propagating through the sensors; and pressure sensors for AC pressures on a silicon diaphragm coated with piezoelectric materials. The piezoelectric effect can also be used to sense small displacements, bending, rotations, and so forth. These measurements require a high input impedance amplifier to measure the surface charges or voltages generated by the strain or stress. Piezoelectric thin films and micromachining technology are used to fabricate strain or stress microsensors of various types.

Piezoresistivity. The piezoresistive effect in conductors and semiconductors is used for commercial pressure sensors and strain gauges. The strain on the crystal structure deforms the energy band structure and thus changes the mobility and carrier density that changes the resistivity or conductivity of the material. The strain in one orientation may affect the conductivity in another orientation. Therefore, similar to the piezoelectric effect, piezoresistivity can be described by an $n \times n$ matrix. For most applications, the piezoresistive material is a crystal and has symmetry in its structure. For cubic crystals, n is 6 (three for axial strain, three for sheer strain, three for voltage, and three for current). Using some simplifying assumptions, the matrix of piezoresistivity coefficients can be reduced to parallel and perpendicular coefficients just as for the piezoelectric coefficients. However, the coefficients are not only orientation dependent, but are also affected by doping and temperature. A practical piezoresistive pressure sensor can be built by fabricating four sensing resistors at the edges or at the center of a thin silicon diaphragm that acts as a mechanical amplifier to increase the stress and strain at the sensor site. Usually, the four sensing resistors are connected in a bridge configuration with push–pull signals to increase the sensitivity. The measurable pressure range for such a sensor can be from 10^{-3} to 10^{6} Torr. Bulk and surface micromachined pressure sensors are currently at various stages of commercialization.

Capacitive/Inductive Impedance. Capacitive or inductive impedances can also be used to measure displacements and strains. Capacitive pressure sensors present some advantages over piezoresistive devices.[11] Capacitive devices integrate the change of elementary capacitive areas, while piezoresistive devices take the difference of the resistance changes of the bridge arms. Therefore, capacitive sensors are less sensitive to the sideways forces and are more stable. Furthermore, capacitive changes can be much larger as a percentage of the reference value than the 5 percent maximum resistance change found in piezoresistive devices. However, capacitive sensors require a capacitance-to-voltage (C-to-V) converter on or near the chip to avoid the effects of stray capacitances.[12] Therefore, the device operation becomes complicated unless the required C-to-V converter can be fabricated on the chip or packaged in the same encapsulation. The measurement circuit also must be stable and have low noise.

Figure 8.5.3 shows a cross-sectional schematic drawing of pressure sensors based on three principles that can be used to measure acceleration, force, flow, and small displacements. Other sensors that can measure torque, rotation, touch, and so forth have also been reported in the literature.

Downloaded from Digital Engineering Library @ McGraw-Hill (www.digitalengineeringlibrary.com)
Copyright © 2004 The McGraw-Hill Companies. All rights reserved.
Any use is subject to the Terms of Use as given at the website.

MICROSENSORS AND MICROACTUATORS

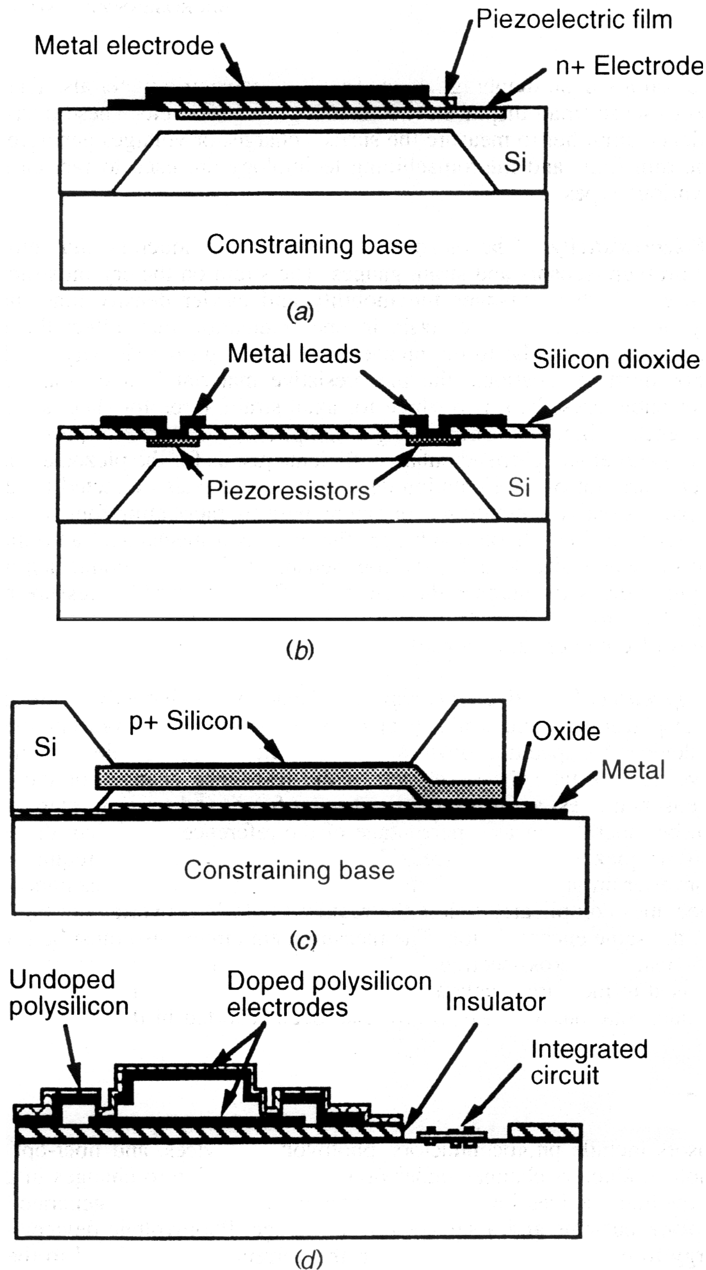

FIGURE 8.5.3 Schematic drawings of the different types of silicon pressure sensors: (*a*) piezoelectric; (*b*) piezoresistive; (*c*) capacitive; and (*d*) surface micromachined capacitive.

Downloaded from Digital Engineering Library @ McGraw-Hill (www.digitalengineeringlibrary.com)
Copyright © 2004 The McGraw-Hill Companies. All rights reserved.
Any use is subject to the Terms of Use as given at the website.

Optical Sensors

Optical sensors include photoconductors, photovoltaic devices, and fiber-optic sensors. The conductivity of photoconductors changes under optical radiation because of changes in the charge carrier population. Photovoltaic devices involve a *p-n* junction where radiation-generated carriers may cross the junction to form currents and a self-generated voltage. Photovoltaic devices, such as solar cells, can supply energy to external circuits. However, the current is proportional to the radiation intensity, but the voltage is not (it is very nonlinearly related to the intensity of the radiation). Many micro-optical sensors and imagers are commercial products now.

When strained, a fiber-optic cable changes the intensity or the phase delay of the output optical wave relative to a reference. Using an optical detector and an interference measuring technique, small strains can be measured with high sensitivity. Intensity sensors can detect changes in optical intensity, which is related to an applied measurand. Examples include: underwater acoustic sensors, fiber-microbend sensors, evanescent or coupled waveguide sensors, moving fiber-optic hydrophones, grating sensors, polarization sensors, and total internal reflection sensors.

Optical interference sensors have been developed for interferometer acoustic sensors, fiber-optic magnetic sensors with a magnetostrictive jacket, and fiber-optic gyroscopes. Specially doped or coated optical fibers have been shown to have great versatility for physical sensors of various types and configurations. They have been used for radiation dosimeters, current sensors, accelerometers, temperature sensors, as well as detectors for liquid level, displacement, strain, torque, and fluid flow. Many chemical and biomedical materials can be sensed with fiber-optic devices.[13]

Magnetic Sensors

Magnetic sensors may employ any of the following effects: (1) the magneto-optic effect based on the Faraday rotation of the polarization plane of linearly polarized light owing to the Lorentz force on bound electrons; (2) the magnetostrictive effect where the magnetic field causes strain on the material; (3) the galvanomagnetic effect that shows up as a Hall field and carrier deflection and magnetoresistance with different sample configurations. Sensing devices include: Hall effect devices—bulk Hall plate and magnetic field sensitive field effect transistors (MAGFETS), magnetotransistors, magnetodiodes, and current domain magnetometers. A comprehensive review paper by Baltes[14] is suggested for further reading.

Future Trends of Physical Sensors

Physical microsensors have been developed over the past 25 years and nearly all possible sensors have been explored. Future research and development will be focused on the following: (1) new materials, principles, and technology that push sensors beyond current limitations, such as high temperature devices, submicron devices, self-powered sensors, etc.; (2) sensor arrays and multiple sensors to improve the sensitivity, selectivity, and stability, as well as to sense the distribution of the measurands; (3) integrated sensors with built-in intelligence to recognize desired signals in noise; and (4) integrated sensors with actuators to provide self-checking and self-calibration functions, as a step toward integrated systems.

CHEMICAL AND BIOMEDICAL MICROSENSORS

General

The introduction of microelectrode assembly and the microfabrication of sensor elements are considered the most significant developments in chemical sensor technology in the past few decades. The potential advantages of microelectrodes for chemical sensor development include: (1) the small electrode size requires a small sample volume, even in biological sensing; (2) the very low level of Faradaic current results in the beneficial effect of very small ohmic potential drop, even in samples of very low conductivity; (3) the limiting current density

Downloaded from Digital Engineering Library @ McGraw-Hill (www.digitalengineeringlibrary.com)
Copyright © 2004 The McGraw-Hill Companies. All rights reserved.
Any use is subject to the Terms of Use as given at the website.

MICROSENSORS AND MICROACTUATORS

increases as the electrode size decreases, thus improving the signal-to-noise ratio, since capacitive background currents are proportional to the surface area; (4) the quick response of microelectrodes allows monitoring of the low-frequency fluctuation of signals and rapid recording of steady-state polarization curves; and (5) the current output of ultramicroelectrodes with dimensions in the μm range is practically insensitive to conventional flow in solution.

Microelectronic fabrication techniques provide advantages for producing these microsize chemical sensors. These include reduced size, reduced sample volume, reduced sensor cost, and fast response. Furthermore, microfabrication processing produces identical, highly uniform, and geometrically well-defined sensor elements. This is particularly attractive for chemical sensors based on the amperometric mode of operation.

While the feasibility and advantages of microfabrication of chemical sensors have been well demonstrated, practical microfabricated chemical microsensors remain elusive. The recent advancements in micromachining technology add new dimensions and impetus to sensor development. These techniques permit the formation of three-dimensional structures and other desirable features and will have a significant and revolutionary impact in future chemical sensor development.[15,16]

Common microfabricated chemical sensors include electrochemical sensors (based on conductivity, potentiometric, and amperometric measurements), tin-oxide based sensors, and calorimetric devices. The operational principles of these sensors are described below.

Electromechanical Sensors

Electromechanical sensors have been used as a whole or as an integral part of many chemical and biosensors. The operational modes of electrochemical sensors are based on traditional laboratory electroanalytical principles. In recent years, the advancement of microelectronic fabrication techniques has provided impetus to the development of new types of electrochemical sensors for chemical and biosensor development. The introduction of solid electrolytes and conductive polymers further enhanced the applicability of electrochemical sensors, particularly in a gaseous environment. A parallel and significant development in sensor technology, though unrelated to conventional electroanalytical principles, is the development of semiconductive chemical sensors, such as the ion-sensitive field effect transistor (ISFET) depicted in Fig. 8.5.4.

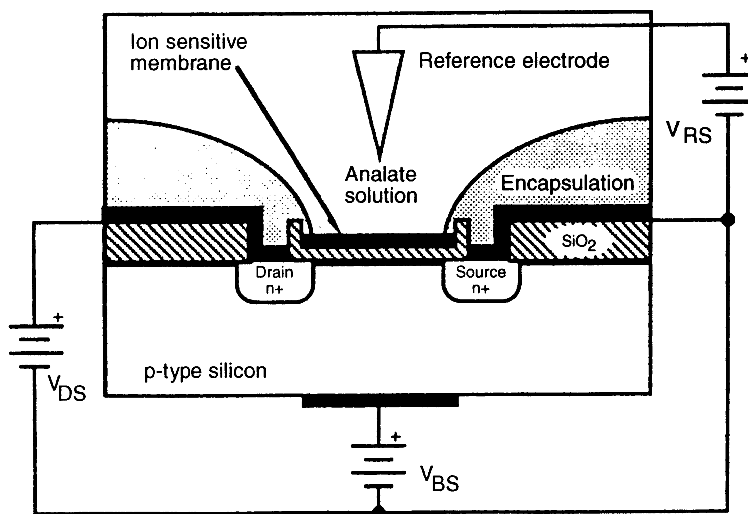

FIGURE 8.5.4 A schematic drawing of a typical ISFET.

Downloaded from Digital Engineering Library @ McGraw-Hill (www.digitalengineeringlibrary.com)
Copyright © 2004 The McGraw-Hill Companies. All rights reserved.
Any use is subject to the Terms of Use as given at the website.

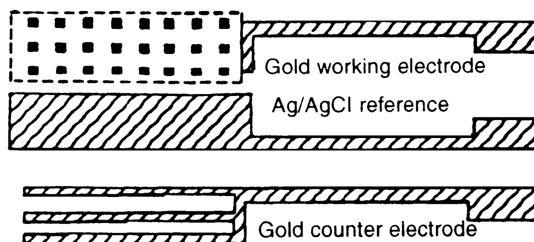

FIGURE 8.5.5 Typical planar, three-electrode electrochemical sensor. The working electrode is divided into many small cells which are in parallel to reduce the effects of flow on the sensor output.

Principles of Electromechanical Sensors. Electromechanical sensors are essential electrochemical cells consisting of two or more electrodes in contact with a solid or a liquid electrolyte. A typical planar, three-electrode electrochemical sensor is shown in Fig. 8.5.5. Electrochemical sensors can be classified according to their mode of operation, e.g., conductivity/capacitance sensors, potentiometric sensors, voltammetric sensors. Amperometric sensors are considered a specific type of voltammetric sensor in this discussion. Measurements of capacitance or resistance, or potential or current of an electrochemical cell, are all feasible. When the cell is used as a sensor, the choice of a measurement parameter is based on the sensitivity, specificity, and accuracy provided with respect to the species to be sensed. Therefore, understanding the principles and limitations of each operational mode is essential in sensor design and development.

Conductivity and Capacitance Electromechanical Sensors. An electromechanical conductivity sensor measures the change in the conductivity of the electrolyte in an electrochemical cell. It is different from the electrical (physical) sensor that measures the change in electrical resistance of the conductor in the presence of a given concentration of a solute. An electromechanical sensor may also involve a capacitive impedance resulting from the polarization of the electrodes and the Faradaic or charge transfer processes.

In a homogeneous electrolytic solution, the conductance of the electrolyte $G(\Omega^{-1})$ is inversely proportional to L (cm), the segment of the solution along the electrical field and directly proportional to $A(\text{cm}^2)$, the cross-sectional area perpendicular to the electric field.

$$G = \sigma \frac{A}{L} \tag{3}$$

where $\sigma(\Omega^{-1}\text{cm}^{-1})$ is the specific conductivity of the electrolyte and is related quantitatively to the concentration and the magnitude of the charges of the ionic species.

The measurement of electrolytic conductance by an electromechanical conductivity sensor employs a Wheatstone bridge with the electromechanical cell (the sensor) forming one of the resistance arms of the bridge. However, the conductivity measurement is complicated by the polarization of the electrodes at the operating voltage. Charge transfer processes occur at the electrode surfaces and a double layer is formed adjacent to each of the electrodes when a potential is imposed on the cell. Both effects can be minimized by using a high-frequency, low-amplitude alternating current. The higher the frequency and the lower the amplitude of the imposed alternating current, the closer the measured value is to the true conductance of the electrolyte. A better technique would be to balance both the capacitance and the resistance of the cell by connecting a variable capacitor parallel to the resistance of the bridge arm adjacent to the cell. The basic measurement could be performed using an impedance measuring bridge in which the resistive and reactive components of the impedance of the electrochemical cell can be determined by balancing the bridge. Greater measurement precision with fewer demands on the operator can be achieved using special electronic instruments, such as lock-in amplifiers, to determine the magnitude of the cell impedance and its phase angle. One way of using the lock-in amplifier is to drive the conductivity cell with a constant current amplitude sinusoidal signal and measure the resulting potential across the cell and its phase angle with respect to the excitation. The impedance magnitude

Downloaded from Digital Engineering Library @ McGraw-Hill (www.digitalengineeringlibrary.com)
Copyright © 2004 The McGraw-Hill Companies. All rights reserved.
Any use is subject to the Terms of Use as given at the website.

MICROSENSORS AND MICROACTUATORS

can then be found by taking the ratio between this measured voltage amplitude and the amplitude of the excitation current.

Potentiometric Sensors. Potentiometric sensors use the effect of the concentration on the equilibrium of the redox reactions occurring at the electrode-electrolyte interface in an electrochemical cell. A potential may develop at this interface as a result of the redox reaction, $Ox + Ze^- = Red$, taking place at the electrode surface, where Ox denotes the oxidant, Red the reduced product, Z the number of electrons in the redox reaction and e^- an electron.

This reaction occurs at one of the electrodes (cathodic reaction in this case) and is called a half-cell reaction. At thermodynamical quasi-equilibrium conditions, the Nernst equation is applicable and can be expressed as

$$E = E^0 + \frac{RT}{ZF} \ln\left(\frac{a_{Ox}}{a_{Red}}\right) \tag{4}$$

where E and E^0 are the electrode potential and electrode potential at standard state, respectively, a_{Ox} and a_{Red} are the activities of Ox and Red, respectively, Z the number of electrons transferred, F the Faraday constant, R the gas constant, and T the operating temperature in Kelvin. In a potentiometric sensor, two half-cell reactions will take place simultaneously. However, only one of the two half-cell reactions should involve the sensing species of interest, and other half-cell reaction is preferably reversible and noninterfering.

Potentiometric sensors can be classified based on whether the electrode is inert or active. An inert electrode provides the surface for the electron transfer or provides a catalytic surface for the reaction and does not actively participate in the half-cell reaction, whereas an active electrode is either an ion donor or acceptor in the reaction. There are three types of active electrodes: the metal/metal ion, the metal/insoluble salt or oxide, and metal/metal chelate electrodes.

Each electrode type can be involved in a chemical cell or concentration cell. In a chemical cell, the two half-cell redox reactions are different. In a concentration cell, the two half-cell reactions are in redox fashion but with different reactant concentrations or activities.

Voltammetric and Amperometric Sensors. Voltammetric measurement is characterized by the current and potential relationship of the electrochemical system, a technique commonly used by electrochemists. This method is often referred to as amperometric measurement. Amperometric sensors can be considered as a subclass of voltammetric sensors, since they are operated in one of the voltammetric modes. In this case, the current-solute concentration relationship is obtained at a fixed potential or overall cell voltage. On the other hand, voltammetric sensors can be operated in other modes such as linear voltammetric or cyclic voltammetric modes. Figure 8.5.6 shows the three different modes of operation and their respective current-potential responses.

Voltammetric sensors utilize the concentration effect on the current-potential characteristics of the electrochemical system for their sensing operation. The current-potential characteristics depend on the rate by which the components in the electrolyte are brought to the electrode surface (mass transfer) and the kinetics of the Faradaic or charge transfer reaction at the electrode surface. Three different modes of mass transfer can be identified in an electrolyte solution, namely, (a) ionic migration as a result of an electric potential gradient, (b) diffusion under a chemical potential difference or concentration gradient, and (c) convective or bulk transfer by virtue of natural convection (density difference) or forced convection.

Linear sweep voltammetry involves increasing the imposed potential linearly at a constant scanning rate from an initial value to a given upper potential limit. The current-potential curve usually shows a peak at a potential where the rate of reaction equals the mass transfer rate. Cyclic voltammetry is similar to the linear sweep voltammetry except that the electrode potential is returned to its initial value at the same scanning rate as shown in Fig. 8.5.6. The cathodic and anodic sweeps would normally generate two current peaks.

Semiconductive Gas-Sensing Microsensors

SnO_2-based Semiconductor Gas Sensors. The surface conductance of semiconducting oxides, such as zinc oxide and tin dioxide, can be influenced by the composition of ambient gases. This phenomenon is the basis of many resistive semiconductor gas sensors.

Downloaded from Digital Engineering Library @ McGraw-Hill (www.digitalengineeringlibrary.com)
Copyright © 2004 The McGraw-Hill Companies. All rights reserved.
Any use is subject to the Terms of Use as given at the website.

MICROSENSORS AND MICROACTUATORS

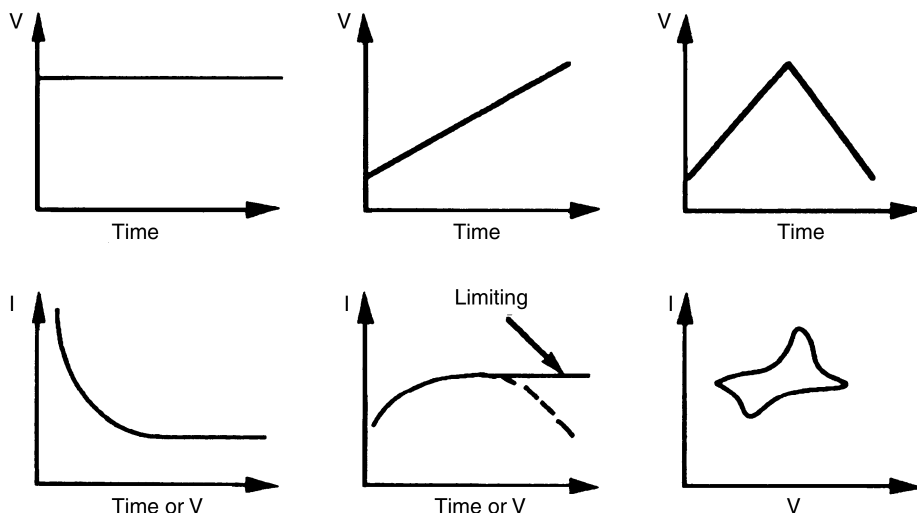

FIGURE 8.5.6 Current-potential relationship of various voltametric modes of operation.

Among the semiconducting oxides, SnO_2 is the most widely used for gas sensors. Such sensors have roles in the detection of flammable or reducing gases such as carbon monoxide, hydrogen and methane at low-level concentrations. SnO_2-based sensors are used to detect leaks of flammable and toxic gases, for combustion control and even for detecting odors. Millions of units of tin dioxide-based gas sensors are sold each year, mainly for automobile exhaust emission monitoring and for gas leak detection. Extensive literature on tin dioxide-based sensors can be accessed.[15,16,21]

As the active sensing part of the gas sensor, tin (IV) oxide (tin dioxide) is nonstoichiometric and is deficient in oxygen atoms. Charge neutrality is maintained by the presence of numbers of tin (II) ions (Sn^{2+}) instead of Sn^{4+} ions, and these Sn^{2+} ions act as electron donors during the process. Thus, the active material of tin dioxide is an *n*-type semiconductor. At elevated temperatures, adsorption of atmospheric oxygen takes place at the face of the tin-oxide film and oxygen accepts electrons that are donated by the *n*-type SnO_2 film and becomes ionic by forming O_2^-, O^-, or O^{2-} anions. If a reducing gas adsorption follows, the reducing gas may react with absorbed oxygen anions and become a positively charged species or the reducing gas may react with the absorbed oxygen atom and release bound electrons. As an example, the overall reaction of carbon monoxide on a tin dioxide film can be described by

$$2e^- + O_2 \leftrightarrow 2O^- \tag{5}$$

$$O^- + CO \leftrightarrow CO_2 + e^- \tag{6}$$

where e^- represents a conduction band electron. In the absence of reducing gas, electrons are removed from the conduction band via the reduction of molecular oxygen and an O^- species is formed such that in consequence the SnO_2 film becomes highly resistive. When carbon monoxide is introduced, it undergoes oxidation to carbon dioxide by surface oxygen anion (O^-) and electrons are reintroduced into the conductive band which leads to an increase in film conductivity. This example provides a general operation principle for tin dioxide-based gas sensors.

The main advantages of tin dioxide-based gas sensors include high sensitivity, low cost, fast response time and low power consumption. However, there are also significant drawbacks, such as long-term drift, relative low selectivity, and effects of humidity and temperature. Efforts have been made in recent years to improve the performance characteristics of tin dioxide-based gas sensors. For instance, noble metal doping of tin dioxide

Downloaded from Digital Engineering Library @ McGraw-Hill (www.digitalengineeringlibrary.com)
Copyright © 2004 The McGraw-Hill Companies. All rights reserved.
Any use is subject to the Terms of Use as given at the website.

MICROSENSORS AND MICROACTUATORS

improves the catalysis process of the detecting gas, which greatly enhances the selectivity and decreases the operating temperature. Other modifications are described later.

Microfabrication of SnO_2-Based Gas Sensors. Fabrication techniques for semiconductive gas sensors have been developed over many years. The microfabrication technologies previously described have added impetus to the advancement of semiconductive gas sensors. The use of microfabrication techniques in the production of tin dioxide type gas sensors provide a good illustration of the potential and future trends of this application.

The original Taguchi type tin dioxide gas sensor was adopted by Figaro Gas Sensor Inc. and by many Japanese groups. The tin dioxide layer is a porous thick film formed by tin dioxide powder sintering. The tin dioxide was prepared from stannic acid gel and followed by firing for 1 h at 500°C. A ratio of palladium and alumina was added to the oxide powder to get the resulting 2:1 ratio of Al_2O_3 to SnO_2. Distilled water was added to the above mixture to yield a paste that was then applied to the surface of an alumina tube with preprinted gold electrodes on the surface. A silica solution was used to cover the paste as a binder. Subsequent low-temperature baking resulted in the formation of a porous sintered thick film. A heater filament was placed inside the tube to provide the required operating temperature.

Thick-Film Technology. Planar thick-film gas sensors have been developed in recent years. The fabrication procedures include sequential screen-printing of thick film gold electrodes, followed by printing a gas-sensitive layer onto an alumina substrate. The paste used for printing of the gas-sensing layer consists of tin dioxide powder along with an organic vehicle and a glass binder. Sometimes a catalytic additive is included. Normally, the thickness of the active film is around several micrometers to tens of micrometers. Schmitte and Wiegleb[17] proposed the composition of tin dioxide paste as 71 percent tin dioxide powder, 5 percent glass powder with solvents and adhesives, and a firing condition of 850°C for 1 hour. A thickness of 15 μm was used for this tin dioxide layer.

The advantages of screen printing technology in the fabrication of thick film gas sensors include the porosity of the sensitive layer, a simple sensor design and a variety of possible geometries for the sensor element (e.g., coplanar, interdigitated, or sandwich form). The heater, located on the back side, is helpful for saving power. The use of thick-film tin dioxide-based gas sensors for the detection of carbon monoxide, hydrogen sulfide, hydrogen, methane, and carbon tetrachloride have been reported.[18]

Thin-Film Technology. This is another useful tool for fabricating tin dioxide-based gas sensors. Chemical vapor deposition (CVD) and reactive evaporation or sputtering can both be applied for this purpose.[19] A typical bulk micromachined, thin film tin oxide gas sensor is shown in Fig. 8.5.7.

Chemical vapor deposition technique involves two gaseous compounds that chemically react and form a compound on the substrate. For the tin dioxide gas sensor film, one of the compounds used is a tin-organic compound (e.g., dibutyl tin diacetate). It is dissolved in an organic solvent and then vaporized at a controlled temperature. The vapor is fed into the reacting chamber using nitrogen as the carrier gas. The tin-organic vapor will react with absorbed oxygen on the surface of the substrate (Al_2O_3 or SiO_2 (Si)) forming the tin dioxide film. A tin dioxide sensitive layer is formed after annealing at 500°C for 12 h or longer. The film thickness and the grain

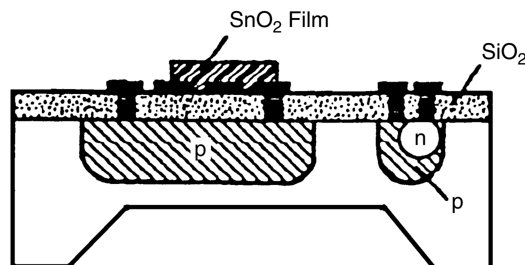

FIGURE 8.5.7 A micromachined tin oxide gas sensor. The tin oxide film is placed on a thin silicon region to reduce the power consumption when the film is heated to its operating temperature.

Downloaded from Digital Engineering Library @ McGraw-Hill (www.digitalengineeringlibrary.com)
Copyright © 2004 The McGraw-Hill Companies. All rights reserved.
Any use is subject to the Terms of Use as given at the website.

MICROSENSORS AND MICROACTUATORS

size of tin dioxide can be controlled by the fabrication conditions and are considered critical for the sensor response. In most cases, the thickness and grain size are in the order of several tens or hundreds of nanometers.

In the reactive evaporation method, the tin dioxide film is fabricated in an evaporator. Pure metallic tin (or tin alloy) is heated to a high temperature (1200–1300°C) and is deposited on a heated substrate on which the sensor heater and gold electrode have already been deposited. After deposition, the sensor unit is annealed in an oxygen-containing atmosphere for several hours at a designated temperature, allowing the tin metal to transform to the oxide. Generally, the resulting thickness of the oxide film is of the order of several hundred nanometers.

Response Characteristics of SnO_2-Based Gas Sensors. *N*-type semiconductive tin dioxide-based gas sensors can be used to detect low-level concentrations of reducing gases such as hydrogen, carbon monoxide, methane, ethanol, hydrogen sulfide, and other inflammable gases, as well as some anesthetic agents like forane, halothane, and ethrane. This sensor is based on the conductance change through the tin dioxide grain boundaries on its surface in the absence of the detecting gas compared with its presence. The sensitivity S of the sensor is expressed as the ratio of the conductivity G under tested gas flow and ambient air, and is expressed as

$$S = G_g/G_a \tag{7}$$

where G_g is the conductivity of the sensor in the presence of tested gas flow and G_a is that in ambient air. The sensitivity of a tin dioxide sensor may be influenced by the layer composition, grain size, operating temperature, humidity, and various other factors.

Calorimetric Sensors

The calorimetric sensor is essentially a high-temperature resistance thermometer that measures the temperature change caused by the heat evolved during the catalytic oxidation of the combustible gases. The most commonly used calorimetric sensors are in the form of an encapsulated platinum coil, which serves both as a heater and as a resistance thermometer. This is normally referred to as a pellistor type calorimetric sensor, and was first developed in 1962. This type of calorimetric sensor can be used for the detection of combustible gas at low concentration. However, the results were not accurate because of the heat loss, a condition that may not be easy to improve with a conventionally sized sensor.

Microfabrication technology provides a means to fabricate miniature calorimetric sensors with improved characteristics. Recently, a thick-film calorimetric microsensor for combustible gas monitoring was fabricated on an alumina substrate.[20] Platinum-thick film was deposited using the screen-printing method. Two types of catalysts were employed, namely, platinum black and palladium. The noncatalytic compensating platinum film was left bare as printed. This microsensor can be used for the detection of hydrogen, carbon monoxide, methane, and ethane. Proper selection of the reaction temperature for catalytic oxidation may lead to possible identification of different gases. Catalytic metallic layer deposition onto silicon wafers or glass plates with the thin-film process has been reported by different groups.[21–24]

A thin-film thermopile sensor based on a bismuth-antimony junction array has been reported.[23] This thermopile consisted of an alternating junction of bismuth and antimony, with a gold contact between, on a kapton thick-film that was formed on a glass plate. Metal shadow masks were used in intimate contact with a kapton sheet to define the geometry for each of the metal layers. The thickness of the bismuth and antimony layer was around 1 μm or less.

An enzyme microsensor based on this thermopile has also been proposed.[24] Glucose oxidase was crosslinked above the active junctions of the thermopile with a thickness of 100 μm. It proved to have a rapid response and good stability when used either intermittently or continuously. Also, catalase and urease were used for immobilization, and both enzyme sensors yield attractive results.

Biosensors

Biosensors are a special class of chemical sensors for molecular detection that take advantage of the high selectivity and sensitivity of biologically sensitive materials. It is a device incorporating a biological sensing element with a traditional sensor, such as physical or chemical sensors. The biological sensing element selectively

Downloaded from Digital Engineering Library @ McGraw-Hill (www.digitalengineeringlibrary.com)
Copyright © 2004 The McGraw-Hill Companies. All rights reserved.
Any use is subject to the Terms of Use as given at the website.

MICROSENSORS AND MICROACTUATORS

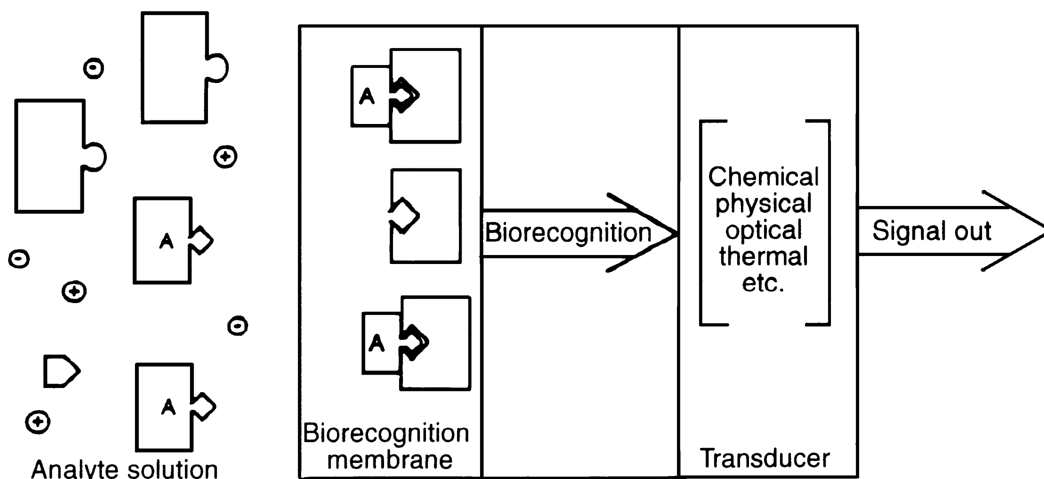

FIGURE 8.5.8 Schematic drawing of the general biosensor. It consists of a traditional transducer with a biological recognition membrane intimately in contact with the transducer. The biologically active material recognizes the analyte molecule, A, through a shape-specific recognition. In affinity-based biosensors, the binding of the analyte and bioactive molecule is the chemical signal that is detected by the transducer. In metabolic biosensors, the biologically active material converts the analyte, and any co-reactants, into product molecules. The transducer converts the result of that reaction into the output signal. The transduction can be through measurement of concentration changes in a product or coreactant concentration, or the heat liberated in the reaction.

recognizes a particular biological material (the measurand) through a reaction, specific adsorption or other physical or chemical process, and the sensor element converts the results of this recognition into a usable signal, usually electrical or optical. Figure 8.5.8 illustrates this definition.

Biosensors represent a specialized field in sensors. A selected reference list is provided.[23–25]

A biological sensor operates on similar principle of a chemical sensor. A biorecognition reaction with the analyte, through a transduction mechanism, results in a sensor output. This output can be electrical, optical, or as a change in color. The biorecognition reaction often involves biocatalysts such as enzymes. The sensory mechanism of a biological sensor is often based on a chemical sensor. Consequently, the microfabricated chemical sensors serve as the bases of microbiological sensors. For instance, the commercially available i-STAT portable clinical analyzer and the portable blood analysis system by Diametrics Medical Inc. are good examples of microchemical sensors serving as the core for biosensor applications.

Measurements of dissolved blood gases (oxygen and carbon dioxide) and blood electrolyte (pH, Na^+, K^+, Ca^{+2}, and others) can be accomplished using electrochemical sensors. For instance, the Clark oxygen sensor for measuring dissolved oxygen in biological fluids is based on an electrochemical-based amperometric sensor. In this electrochemical sensor, the reduction of oxygen results in a cathodic current, which can then be used to quantify the oxygen presented. This approach is applicable to measurements of dissolved oxygen in biological samples. Therefore, miniaturization of electrochemical sensors or chemical sensors can lead to the development of microsize biological sensors making portable biological analyzers a reality.

Biological sensors based on enzymatic reactions also frequently use a chemical sensor as the sensing mechanism. For example, a blood glucose sensor employs glucose oxidase to catalytically oxidize the glucose in the presence of oxygen. One of the resulting products is hydrogen peroxide, which can be detected electrochemically. The amount of hydrogen peroxide detected can then be used to quantify the blood glucose presented. Other enzymatic reactions have also been used for extensive biological sensor development, and the detection of a product or a co-reactant with a chemical or electrochemical sensor is then used to quantify the bio-analyte.

As anticipated, the application of MEMS technology to chemical sensors leads to the logical consideration of using MEMS technology in the development of biological sensors.[20,21] Many attempts in this direction have been made but with only limited success thus far. The fragility and relatively poor biocompatibility of silicon

Downloaded from Digital Engineering Library @ McGraw-Hill (www.digitalengineeringlibrary.com)
Copyright © 2004 The McGraw-Hill Companies. All rights reserved.
Any use is subject to the Terms of Use as given at the website.

are concerns. Furthermore, biological sensors often prefer to be disposable or to have a limited number of uses. This is difficult to achieve with expensive MEMS manufacturing processes.

MEMS technology applied to biomedical fields has led to the term BIOMEMS. Major efforts in BIOMEMS are focusing on DNA chips and drug delivery systems. These applications are beyond the scope of biological sensors for in vivo and in vitro applications. Development of biological sensors is a vast scientific endeavor. It is beyond the scope of this chapter to discuss it in detail. We wish only to point out the relationship between chemical and biological sensors, and the issues involved in MEMS technology to both types of microdevices.

Laboratory on a Chip. One of the potential applications of MEMS technology is that of a complete chemical laboratory on a chip (LOC). The functional components of a simple analytical laboratory would be fabricated using silicon-based microfabrication technology. These functional components might include sample pretreatment, transportation, and separation of the sample, introduction of reagents, sensing and detection and data collection and analysis. The advantages of an LOC approach include the requirement of a small sample volume, minimum quantity of expensive reagents, and relatively portability. However, its success depends on many intricate microfabricated components such as microfluidic devices, micropumps, valves, channels, and sensors. *Fundamentals of Microfabrication* by M. Madou provides a summary of the commercial aspects of this technology. The transport properties of fluid in these microstructures can differ significantly from those in a larger-size environment. Fabrication costs are again an issue.

The term "μTAS," meaning "micro total analytical system," is used in the MEMS field. It is a part of the "system on a chip" when applied to the integrated biochemical analytical systems. The term biochip also is being used in popular science and news media in reference to the biomedical diagnostic systems fabricated on a chip.

Chemical and Biosensor Packaging

Packaging of chemical sensors is a critical issue that needs to be addressed. Differing from the packaging of electronics, that of chemical sensors must provide an area where the sensor is exposed to the environment. This means that on one hand the overall integrity of the sensors must be protected, yet on the other hand, the most critical part of the sensor must be exposed to the sensing environment, which can often be hostile. There is no simple or direct packaging method for chemical sensors, rather, it depends on the environment of the sensor applications, such as high temperature or the presence of corrosive materials.

MICROACTUATORS

Research on design, fabrication, and characterization of new microactuators is accelerating. A critical need is the development of actuation forms that are compatible with the materials and processing technologies of silicon microelectronics. Additionally, actuation is to be powered and controlled electrically, allowing full utilization of integration with on-chip electronics. Despite these stringent requirements, numerous physical phenomena have been demonstrated for microactuator applications.[26] However, the most commonly used microactuation methods have so far been either electromagnetic or thermal and are, therefore, the microactuation techniques described in this section as examples. Other microactuation techniques can be found in the journals and proceedings of the conferences in the field (see Bibliography).

Selected microactuators that exemplify the basic microactuator concepts and mechanical designs are described here. Two basic electrostatic microactuator designs, lateral resonant devices and micromotors, are discussed in more detail as examples.

Mechanical Design of Microactuators

The mechanical design of microactuators can be divided into two classes: (1) mechanisms and (2) deformable microstructures. Mechanism-type microactuators (e.g., the micromotor shown in Fig. 8.5.9) provide displacement

Downloaded from Digital Engineering Library @ McGraw-Hill (www.digitalengineeringlibrary.com)
Copyright © 2004 The McGraw-Hill Companies. All rights reserved.
Any use is subject to the Terms of Use as given at the website.

MICROSENSORS AND MICROACTUATORS

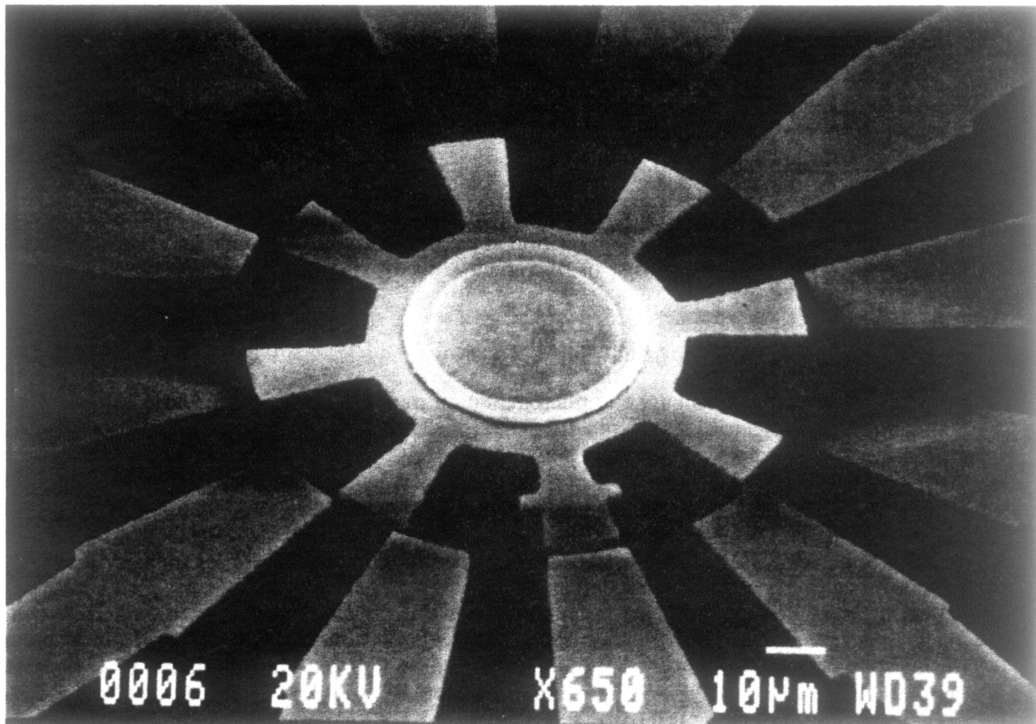

FIGURE 8.5.9 A photomicrograph of a salient-pole, variable-capacitance, side-drive micromotor. The rotor rotates in the plane of the motor/substrate.

and force through rigid-body motion while deformable microstructures (e.g., beams, diaphragms, and the lateral resonant microactuator of Fig. 8.5.10) provide displacement and force through mechanical deformation (or straining). The unrestrained, large motion capability of mechanism-type microactuators comes at the cost of friction, which is present in the bearings and joints of such devices. In contrast to the operation of macroscopic mechanical devices in which gravitational and inertial forces are often dominant, friction plays an important role in the operation of micromechanical devices. In micromechanical devices, gravitational forces (i.e., weight of the moving parts) are usually insignificant while inertial forces are often, but not always, negligible. Deformable microstructures eliminate friction since they only use joints and suspensions. Avoiding friction, however, comes at the cost of restrained (and often small) motion.

Electromagnetic and Thermal Microactuation

Most notable among electromagnetic microactuation methods have been electric (often referred to as electrostatic), piezoelectric, and magnetic actuation. Utilization of electrostatic actuation in microfabricated mechanical devices is readily possible since IC processes provide a wide selection of conductive and insulating materials. By using the conductors as electrodes and the insulators for electrical isolation of the electrodes, attractive electrostatic forces can be generated by applying a voltage across a pair of electrodes. To generate repulsive forces, *electrets* (dielectric materials that have a permanent charge) are required; however, electrets are not readily available in the IC industry and, as a result, have not as yet been used in microactuation.

Downloaded from Digital Engineering Library @ McGraw-Hill (www.digitalengineeringlibrary.com)
Copyright © 2004 The McGraw-Hill Companies. All rights reserved.
Any use is subject to the Terms of Use as given at the website.

MICROSENSORS AND MICROACTUATORS

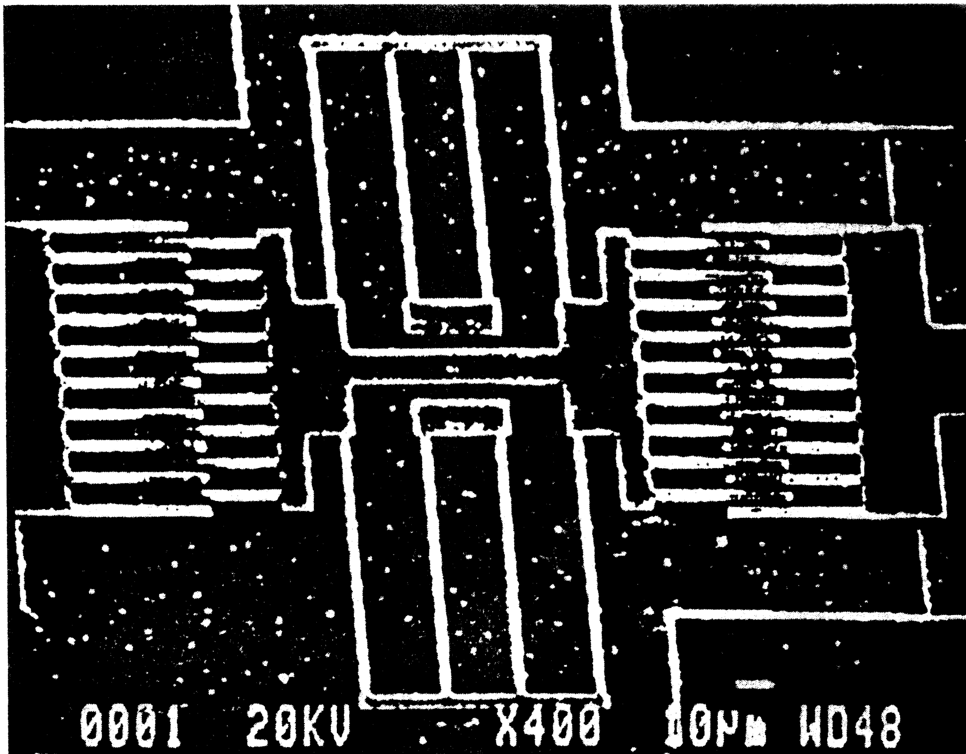

FIGURE 8.5.10 A photomicrograph of a lateral resonant device. The shuttle mass attached to the folded cantilever suspension moves in the plane of the device/substrate in the direction of the comb fingers.

Electrostatic forces can be used in conjunction with conventional deformable microstructures such as beams and diaphragms to generate force or provide motion. For this group of microactuators, the deformation is predominantly in the direction normal to substrate plane. Figure 8.5.11 is a schematic example of an electrostatic diaphragm microactuator. By applying a voltage across the diaphragm/electrode air gap (which is typically a few microns), the diaphragm can be deflected upward. The generated electric force results from the attractive force between the electrical charges of opposite sign on the electrically conductive silicon surfaces across the gap. As in the case of the lateral resonant microactuator in Fig. 8.5.11, electrostatic actuation can also be used in conjunction with deformable microstructures to provide motion in the plane of the substrate.

Electrostatic actuation can also be used in conjunction with a mechanism, for example, in the case of the micromotor in Fig. 8.5.9. In an electric micromotor, the attractive forces generated by electric charge distributions are used to convert electrical to mechanical energy. By proper commutation of these charge distributions (i.e., proper switching of excitation voltage) on a set of stationary electrodes, known as the stator, and a set of moving electrodes, known as the rotor, continuous motion of the rotor can be achieved.

Another form of microactuation has been based on the piezoelectric effect. Figure 8.5.12 is a schematic example of a possible cantilever microactuator design. In this design the piezoelectric thin film, which is sandwiched between two electrodes, is placed on top of a silicon cantilever beam. When a voltage is applied across the piezoelectric film, the film will expand or contract in the lateral direction, resulting in a downward or upward deflection, respectively, of the cantilever. The polarity of the applied voltage determines if the film expands or contracts. Piezoelectric films have been used to provide actuation in a variety of applications such

Downloaded from Digital Engineering Library @ McGraw-Hill (www.digitalengineeringlibrary.com)
Copyright © 2004 The McGraw-Hill Companies. All rights reserved.
Any use is subject to the Terms of Use as given at the website.

MICROSENSORS AND MICROACTUATORS

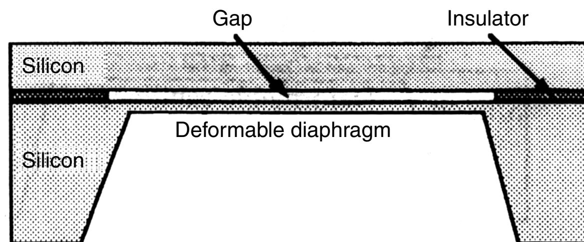

FIGURE 8.5.11 A schematic drawing of an electrostatic diaphragm microactuator.

as valves, pumps, positioning devices, and ultrasonic micromotors.[27,28] Typical piezoelectric thin films being used in microactuators are zinc oxide (ZnO), lead zirconate titanate (PZT), and polyvinylidene difluoride (PVDF). Of these materials, PZT has the largest piezoelectric coefficients.

Similar to electrostatic actuation, magnetic actuation can be used in conjunction with both deformable microstructures and mechanisms. Since most macroscopic electromagnetic motors use magnetic actuation, this form of actuation is most familiar. However, its utilization for microfabricated actuators has been limited because it requires magnetic materials and fabrications of windings. Nevertheless, a few studies[29–31] have addressed the development of magnetic microactuators. For example, magnetic micromotors made of nickel have been demonstrated by using the LIGA fabrication process.[32]

While electromagnetic microactuation has been demonstrated in conjunction with both classes of microactuators, thermal microactuation is primarily suitable for deformable microstructures. Most notable among thermal microactuation methods have been bimetallic, shape memory alloy (SMA), and thermopneumatic. Figure 8.5.13 shows a schematic example of a possible bimetallic or SMA cantilever microactuator. Bimetallic microactuators use the thermal coefficient of expansion mismatch between the material components of a sandwich layer to generate force or motion.[33] For example, applying a current through the heating resistor in the device of Fig. 8.5.13 will heat the composite metal/silicon cantilever beam. Since the metal expands more than the silicon, the beam will deflect downward. The downward deflection of the beam can be maintained by supplying power through the heating resistor. Since microfabrication techniques lend themselves more easily to the stacking of the materials on top of rather than beside each other, reported microactuators based on the bimetallic effect provide deformations that are predominantly in the direction normal to the plane of the substrate.

SMAs are metals that have shape-recovery characteristics. When these alloys are plastically deformed at one temperature (martensitic phase), they will completely recover their original shape on being raised to a higher temperature (austenitic phase).[34] In recovering their shape, the alloys can produce a displacement or force, or a combination of the two, as a function of temperature. The development of thin-film SMAs provides the potential for development of silicon-based MEMS that incorporate SMA microactuators. The specific SMA that has been studied for microactuator applications is Nitinol or TiNi, an alloy of titanium and nickel.[35,36] TiNi alloys undergo a martensitic transformation during cooling at a temperature M_s, and the transformation is completed at a lower temperature M_f. In the temperature interval between M_s and M_f, the alloy

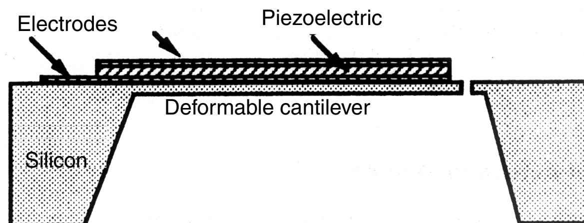

FIGURE 8.5.12 Schematic of a piezoelectric cantilever microactuator.

Downloaded from Digital Engineering Library @ McGraw-Hill (www.digitalengineeringlibrary.com)
Copyright © 2004 The McGraw-Hill Companies. All rights reserved.
Any use is subject to the Terms of Use as given at the website.

MICROSENSORS AND MICROACTUATORS

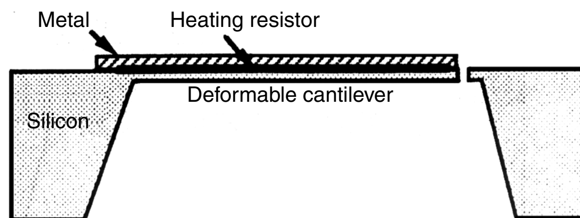

FIGURE 8.5.13 Schematic drawing of a bimetallic or shape-memory-alloy cantilever microactuator.

has a two-phase (austenite and martensite) microstructure; the transformation temperature is relatively narrow and is on the order of 15°C.[37,38] Therefore, one may speak of a transition temperature, M_t (average of M_s and M_f), below which the alloy shows the shape memory effect and above which the effect is absent. Associated with the martensitic transformation, TiNi shows a shape memory effect.

An SMA cantilever microactuator based on the construction shown in Fig. 8.5.13 would, for example, use TiNi for the metal component. Assume that the cantilever is fabricated such that it is flat (i.e., no deflection) with TiNi in its austenitic phase (well above M_t), and then cooled to below M_t to form the martensitic phase. Since the cantilever is also a bimetallic device, it will deflect upward on cooling (i.e., TiNi contracts more than the silicon). By applying current through the heating resistor, the cantilever will try to recover its flat shape once M_t is reached. Note that there would be some bimetallic contribution to the actuation until M_t is reached. However, the transition at M_t will be sudden and because of the shape memory effect.

In a thermopneumatic microactuator, the volume expansion of a fluid is used for actuation.[39] Figure 8.5.14 is a schematic of a possible implementation of a thermopneumatic diaphragm microactuator based on resistive heating of a fluid in a micromachined sealed cavity. As the fluid is heated, its volume expands, increasing the pressure inside the cavity. The increased pressure acts as a load on the thin diaphragm and results in its deflection. The fluid may be a liquid that turns to a gas or simply a gas that expands on heating.

Comparison of Actuation Methods

It is often of interest to compare the various microactuation methods for their relative advantages and disadvantages, but detailed comparisons are only realistic when performed in light of an application. Nevertheless, it is possible to outline some general points. An important point of interest for a microactuation method is the amount of force (or mechanical energy) that can be generated. One approach for general comparison is to estimate the amount of energy, W, available per unit volume. For example, the energy per unit volume, W, available from a TiNi SMA material can be calculated from the area under the operating curve on the stress-strain

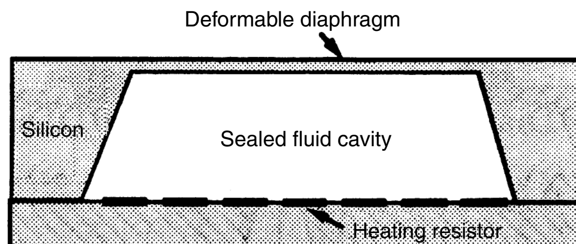

FIGURE 8.5.14 Schematic of a thermopneumatic diaphragm microactuator.

Downloaded from Digital Engineering Library @ McGraw-Hill (www.digitalengineeringlibrary.com)
Copyright © 2004 The McGraw-Hill Companies. All rights reserved.
Any use is subject to the Terms of Use as given at the website.

MICROSENSORS AND MICROACTUATORS

diagram. For an austenitic state with a yield strength of 420 MPa and an available shape memory strain of 8 percent, W is 4×10^7 J/m^3. For bimetallic actuators, W would depend on the magnitude of temperature change but can be of comparable magnitude. For an electrostatic microactuator, $W = (1/2)\epsilon_0 E_{max}^2$ is nearly 4×10^5 J/m^3, assuming an electric field breakdown limit (E_{max}) of 3×10^8 V/m for microscopic air gaps.[40] (ϵ_0 is the permittivity of free space.) For piezoelectric microactuators, W may be up to 10^5 J/m^3, assuming PZT to be the piezoelectric material. For magnetic microactuators, $W = (1/2)(B_{max}^2/\mu_0)$ is about 10^6 J/m^3, assuming a magnetic flux density saturation of 1.5T.[40] (μ_0 is the permeability of free space.)

Other factors must also be considered in comparing different microactuation methods. In general, thermal microactuators have a slow response time (e.g., on the order of tens of milliseconds) and high power consumption (e.g., on the order of tens of milliwatts). Comparatively, electromagnetic microactuators can be much faster (e.g., microsecond response time) and consume far less power, particularly electrostatic microactuators. The construction of thermal microactuators often requires the final freestanding part to be a laminate of layers with very different mechanical properties. This often complicates device design as evidenced by the fact that reported bimetallic actuators exhibit a preset deflection because of the residual stresses in the thin films. Piezoelectric microactuators require deposition of additional films since silicon is not piezoelectric. Furthermore, static operation of piezoelectric microactuators is limited by charge leakage. Electrostatic microactuators can be fabricated using conducting and insulating films that are common to microelectronics technology. Static excitation of electrostatic microactuators requires voltages across insulating gaps and nearly no loss. Magnetic microactuators require magnetic materials that are not common in IC technology and often require some type of manual assembly. Static excitation of magnetic microactuators requires current through windings and persistent conduction losses.

Microactuator Examples

While research and development of microactuators has been rapidly expanding in the last few years, the four classes of microactuators described below are representative of a large segment of the microactuator technology. The examples provide typical performance characteristics of a large cross section of microactuators.

Microvalves. Microactuator technology is being pursued for the development of microvalves for industrial (e.g., electronic pressure regulators) and biomedical applications (e.g., drug delivery and chemical analysis fluidic microsystems). The microvalve in Fig. 8.5.15 is an example of a bimetallic microactuator fabricated by bulk micromachining and bonding of two wafers.[41] Heating of the bimetallic diaphragm by passing a current

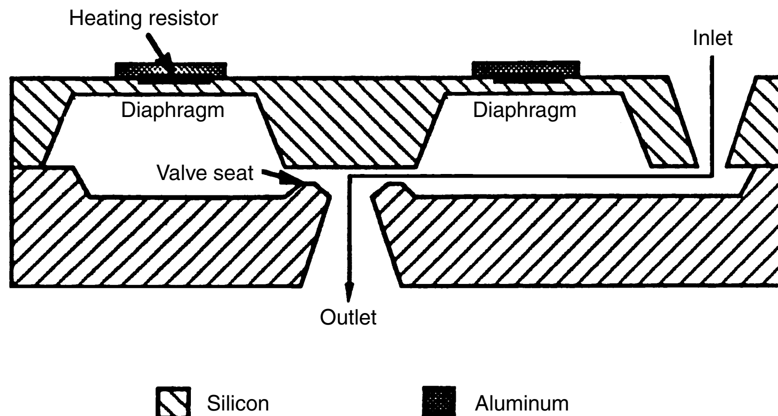

FIGURE 8.5.15 Schematic drawing of a bimetallic microvalve.[21]

Downloaded from Digital Engineering Library @ McGraw-Hill (www.digitalengineeringlibrary.com)
Copyright © 2004 The McGraw-Hill Companies. All rights reserved.
Any use is subject to the Terms of Use as given at the website.

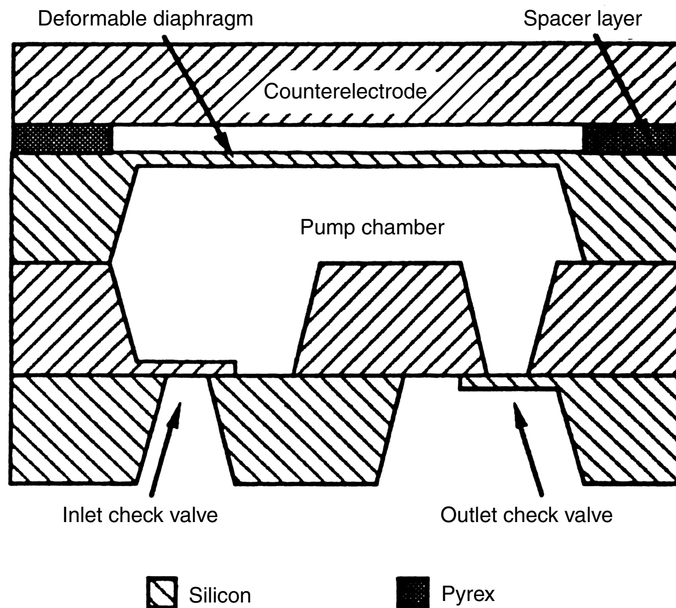

FIGURE 8.5.16 Schematic drawing of an electrostatic micropump.[43]

through a heating resistor embedded between the metal and silicon sandwich causes the metal and silicon layers to expand. This expansion results in the downward deflection of the diaphragm because of the mismatch in the thermal expansion coefficients of the metal and silicon. If heated sufficiently, the diaphragm can deflect far enough to close off the valve. The diaphragm in this device is 2.5 mm in diameter and is 10 μm thick. A 5 μm-thick aluminum layer is used as the metal component. Fully proportional control of flows in the range of 0 to 300 cc/min has been demonstrated with this valve for input pressures from zero to 100 psi. On/off flow ratios have been greater than 1000. To close the valve at 20 psig input, 1.5 W of power is required.[41]

Electrostatic, shape memory metal (SMA)[42] and thermopneumatic[39] actuations are also being used in the development of microvalves similar in architecture and concept to that described above.

Micropumps. Another application of microactuator technology is the development of micropumps. Such micropumps are of interest, for example, in developing chemical analysis and drug delivery microsystems. The micropump in Fig. 8.5.16 is an example of electric actuation in conjunction with a deformable diaphragm.[43] This micropump employs two check valves that are simply cantilever beam flaps covering micromachined holes. When a voltage is applied to the counter electrode, the diaphragm deflects up, increasing the pump chamber volume and reducing its pressure. The inlet check valve then opens as its cantilever flap bends up in response to differential pressure. When the excitation is turned off, the diaphragm returns to its normal position, reducing the pump chamber volume and increasing its pressure. The outlet valve then opens allowing the fluid to exit. In the micropump described, the square diaphragm is 4×4 mm^2 and 25 μm thick; the actuator gap is 4 μm. Pumping has been demonstrated for actuation frequencies of 1 to 100 Hz. At 25 Hz, a pumping rate of 70 μl/min has been demonstrated when the outlet and inlet pressures are equal. Typical forward to reverse flow rate ratio of the check valves is 5000:1.[43]

Lateral Resonant Devices. Where the deformable microactuators above were fabricated by bulk micromachining and bonding, many current deformable microactuators rely on (polysilicon) surface micromachining. Lateral resonant microstructures are the newest among these;[44] they are actuated by electrostatic forces. Figure 8.5.17 shows a plan-view schematic of the lateral resonant microactuator of Fig. 8.5.10. While

Downloaded from Digital Engineering Library @ McGraw-Hill (www.digitalengineeringlibrary.com)
Copyright © 2004 The McGraw-Hill Companies. All rights reserved.
Any use is subject to the Terms of Use as given at the website.

MICROSENSORS AND MICROACTUATORS

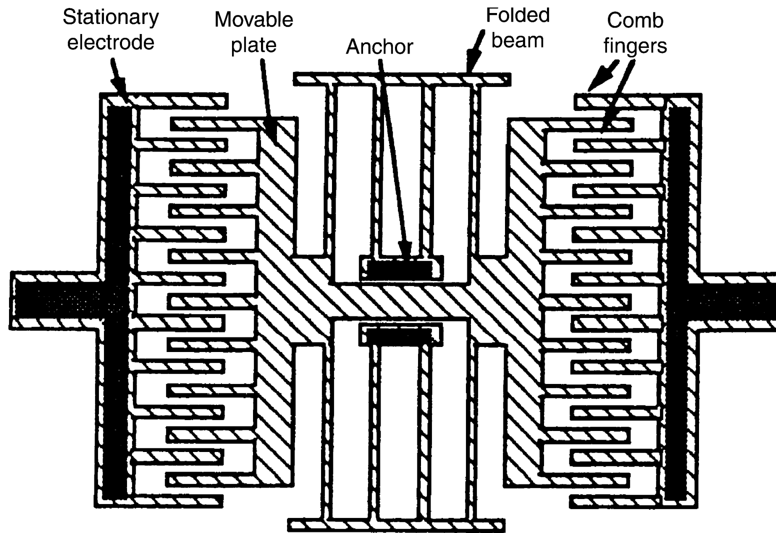

FIGURE 8.5.17 Plan view of a lateral resonant microactuator.

polysilicon surface micromachining has thus far been the primary technique for the fabrication of these devices, other fabrication techniques are emerging.[45] Lateral resonant structures typically consist of a movable plate that is suspended a couple of microns above the substrate by a flexible folded beam support. The folded beam support is anchored to the substrate at one end and attached to the movable plate at the other end. (In Fig. 8.5.17, the light-fill regions indicate parts that are suspended over the substrate and the dark-fill regions indicate the substrate anchor areas.) Electric forces through the use of comb-drive and/or side-drive electrodes are employed to provide actuation. The suspension and actuation are designed for lateral deformation of the suspension and, therefore, lateral movement of the movable plate. In resonant mode, these microactuators can provide lateral deformations near 10 μm; tens of kHz is typical of resonant frequencies for the designs reported.[44]

The electrostatic force generated by a single comb finger on the movable plate is

$$F = 2\epsilon_0 V^2 \left(\frac{t}{g}\right) \tag{8}$$

where F = force
ϵ_0 = permittivity of free space
V = applied voltage
t = beam thickness
g = comb finger gap

The factor of 2 accounts for the fact that on the stationary electrode there are always two comb fingers, one on each side of the comb finger on the movable plate. The above formula is based on simple parallel-plate capacitance calculations. For comparable values of t and g (which is often the case in actual devices based on polysilicon surface micromachining), the above formula provides a reasonable approximation. Its accuracy increases as the t to g ratio increases beyond 3 to 4 such that the contribution of the fringing fields becomes negligible. For t to g ratios below 1, the accuracy of the above formula may be quite poor.

This displacement x (along the comb finger direction) of the movable plate as a function of the applied force is

$$x = \frac{F}{K} \tag{9}$$

Downloaded from Digital Engineering Library @ McGraw-Hill (www.digitalengineeringlibrary.com)
Copyright © 2004 The McGraw-Hill Companies. All rights reserved.
Any use is subject to the Terms of Use as given at the website.

MICROSENSORS AND MICROACTUATORS

TABLE 8.5.1 Typical Lateral Resonant Device Parameters

Parameter	Typical values
Comb finger gap (μm)	1–4
Comb finger width (μm)	2–4
Number of fingers	9–11
Finger length (μm)	20–40
Polysilicon thickness (μm)	1.5–3
Beam length (μm)	80–200
Beam width (μm)	1–2

where x is the displacement of the shuttle, and K is the mechanical stiffness of the folded beam suspension. The stiffness of the suspension is given by

$$K = 2Et\left(\frac{w}{l}\right)^3 \tag{10}$$

where E = Young's modulus (near 160 GPa for polysilicon)
υ = Poisson's ratio (assumed to be near 0.3 for polysilicon)
l = beam length
w = beam width

When the t to w ratio is greater than 1, wide beam effect can be accounted for by dividing the modulus by $(1 - \upsilon^2)$. The resonant frequency of the shuttle is given by

$$f = \frac{1}{2\pi}\sqrt{\frac{K}{M}} \tag{11}$$

where M is the mass of the shuttle.

Typical dimensions of lateral resonant devices are described in Table 8.5.1. Based on these typical dimensions, the generated forces per square volt, for a single comb finger, are usually in the range of 4 to 26 pN/V^2, while typical stiffness values for the suspension are in the range of 60 mN/m to 15 N/m.

To improve performance by increasing the generated actuation force[46] and displacement,[47] other polysilicon deformable microstructure mechanical designs that use electrostatic actuation have been tried. The reader is referred to the proceedings of recent conferences in the field for reported design variations.

Micromotors. In addition to deformable microstructures, MEMS require large-motion actuators (e.g., micromotors) to power linkages. Electrostatic actuation in conjunction with polysilicon surface micromachining has been used to develop variable-capacitance side-drive micromotors[48] similar to the one shown in Fig. 8.5.9. For variable-capacitance micromotors (which require conductive materials for the rotor and the stator, as well as insulators for electrical isolation), the material requirements are compatible with polysilicon surface micromachining. Heavily-phosphorous-doped polysilicon is used for the rotor and the stator, and silicon nitride is used for electrical isolation. Additionally, since the electric breakdown limit in air increases drastically for microscopic (order of 1 μm) air-gap sizes, high enough torques can be generated to start the motor. The electric field breakdown limit in air is 3×10^6 V/m for macroscopic dimensions and increases to above 10^8 V/m for microscopic, air-gap sizes.[44,49] For microscopic dimensions, the gap size approaches the mean free path in air. As a result, the field strength increases since avalanche breakdown, which is the field breakdown mechanism, requires a large number of collisions to ionize the air.

Figure 8.5.18 is a plan-view schematic of the micromotor in Fig. 8.5.9 and describes the micromotor operation. At the end of a phase excitation, the rotor is fully aligned with the excited stator phase (e.g., the configuration shown in Fig. 8.5.18 for alignment of rotor pole set 1 with stator phase B). To move the rotor clockwise,

Downloaded from Digital Engineering Library @ McGraw-Hill (www.digitalengineeringlibrary.com)
Copyright © 2004 The McGraw-Hill Companies. All rights reserved.
Any use is subject to the Terms of Use as given at the website.

MICROSENSORS AND MICROACTUATORS

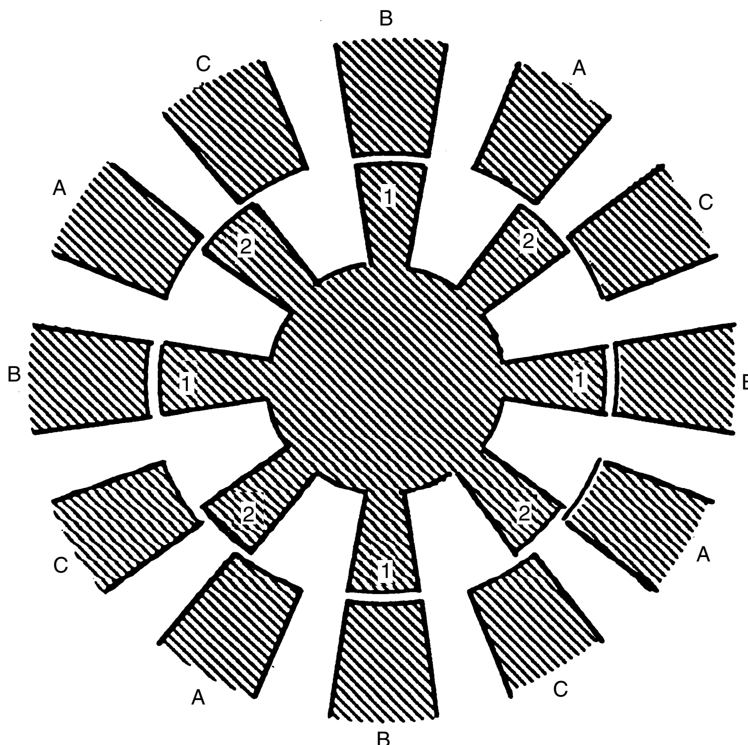

FIGURE 8.5.18 Plan-view schematic of the micromotor shown in Fig. 8.5.9.

stator phase C is excited next. To move the rotor counterclockwise, stator phase A would be excited next. Proper commutation of the excitation signal results in continuous rotation of the rotor. The operation of these micromotors relies on the storage of electrical energy in a variable rotor-stator capacitance. The change in this capacitance in the direction of motion is proportional to the output torque of the micromotor. In terms of design, one strives for optimum torque generation by enhancing the capacitance change in the direction of motion. Very rough estimates of the micromotor motive torque can be calculated by parallel-plate approximations. More accurate calculations of torque have been performed by finite element analysis.[50]

A detailed discussion of the evolution of polysilicon micromotors in terms of design and operational characteristics is documented elsewhere,[51–55] and a review of the micromotor technology is available in Ref. 49. In sum, the evolution in the design of variable-capacitance micromotors has been motivated by enhanced rotor stability, simpler fabrication processes, and increased torque. The former two are achieved at the cost of sacrificing the latter by using the side-drive architecture shown above. Some of the torque is regained by going from a salient-pole to a wobble (Fig. 8.5.19) micromotor design.[49,51,52,55] The structural design of a wobble micromotor is identical to that of the salient-pole (see Fig. 8.5.20) showing the micromotor cross-section), except that the rotor and stator designs are different. For the wobble micromotor, the rotor has no poles (or no saliency). The central feature of the wobble micromotor is that the rotor wobbles around the center bearing post as the excitation voltage is moved on the stator poles. Since there is a finite bearing clearance, the rotor's wobbling motion will also result in a rotation of the rotor.

Table 8.5.2 presents typical dimensions of electrostatic polysilicon micromotors. The reader is referred to Refs. 51, 53, and 56 for a detailed discussion of micromotor design and to Ref. 49 for a review of the micromotor technology.

Micromotor operation has been demonstrated in dielectric liquids (e.g., deionized water and silicone oil),[57] as well as in gaseous environments (e.g., nitrogen, argon, oxygen, and room air).[58] The performance and

Downloaded from Digital Engineering Library @ McGraw-Hill (www.digitalengineeringlibrary.com)
Copyright © 2004 The McGraw-Hill Companies. All rights reserved.
Any use is subject to the Terms of Use as given at the website.

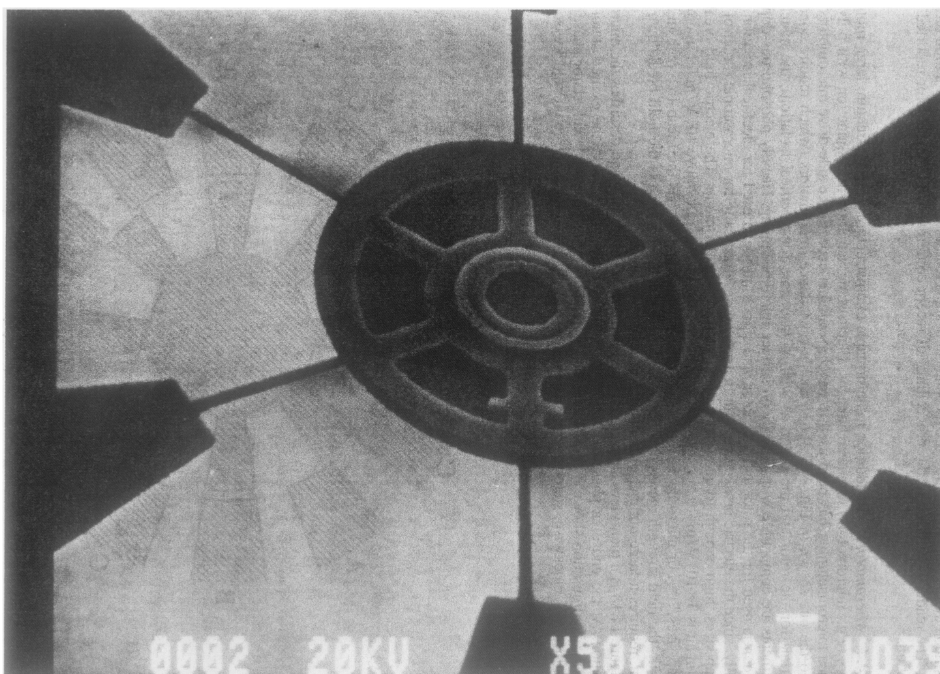

FIGURE 8.5.19 A photomicrograph of a wobble micromotor having a 100-μm diameter.

lifetime of micromotors have been improved significantly over time. Excitation voltages as low as 30 V have been sufficient in operating some current micromotors.[57,58] Open-loop operational stepping speeds up to 15,000 rpm have been reported for operation in a gaseous environment.[51,57] The maximum attainable speeds for operation in gaseous environments have been limited by the power supply and not the micromotor. Micromotor lifetime has been extended to many millions of cycles over a period of several days for operation in room air or silicone oil.[55,57] For these micromotors, a clear failure point has not yet been identified even though some micromotors have been tested for a few hundred million start-stops. Dynamic friction torque is below 10 percent of the micromotor motive torque[54] and wear is not presently a limiting factor in micromotor operation.[55] The motive torque of the side-drive micromotors is typically on the order of tens of pico-Newton-meters (pN-m).

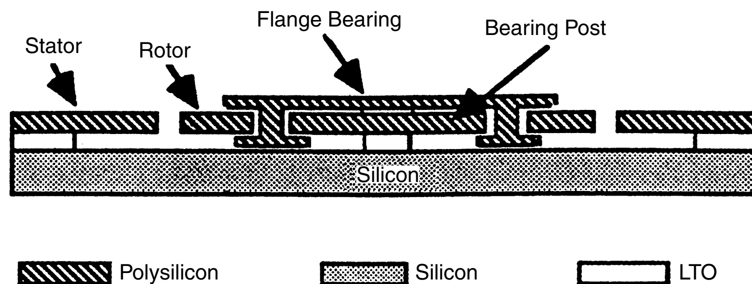

FIGURE 8.5.20 Schematic drawing of the cross section of salient-pole and wobble micromotors of Figs. 8.5.9 and 8.5.19.

Downloaded from Digital Engineering Library @ McGraw-Hill (www.digitalengineeringlibrary.com)
Copyright © 2004 The McGraw-Hill Companies. All rights reserved.
Any use is subject to the Terms of Use as given at the website.

TABLE 8.5.2 Typical Micromotor Dimensions

Parameter	Value
Rotor/stator gap (μm)	1.5–2.5
Rotor inner radius (μm)	10–20
Rotor outer radius (μm)	50–75
Bearing clearance (μm)	0.3–0.8
Rotor to substrate gap (μm)	2–2.5

REFERENCES

MEMS Technology

1. Muller, R. S., et al. (eds.) "Microsensors," *IEEE Press*, 1991.
2. Petersen K. E., "Silicon as a mechanical material," *Proc. IEEE*, 70, p. 420, 1982.
3. Mehregany, M., W. H. Ko, A. S. Dewa, and C. C. Liu, "Introduction to MEMs and Multiuser MEMs Processes," Case Western Reserve University, Short Course Handbook, <http://mems.cwru.edu/shortcourse/partITOC.html>.
4. Ko, W. H., J. T, Suminto, and G. J. Yeh, "Bonding Techniques for Microsensors," in Micromachining and Micropackaging of Transducers, C. D. Fung et al. (eds.), Elsevier, pp. 41–46, 1985.
5. Tong, Q. Y., and U. Gosele, "Semiconductor Wafer Bonding," Wiley, 1999.
6. Gui, Cheng-Qun, "Direct Wafer Bonding with Chemical Mechanical Polishing," Ph.D. Thesis, University of Twente, 1998.
7. Menz, W., W. Bacher, M. Harmening, and A. Michel, "The LIGA technique—a novel concept for microstructures and the combination with Si-techniques by injection molding," *MEMS* 90, p. 69, 1990.
8. Frozier, A. B., and M. G. Allen, "High aspect ration electroplated microstructures using a photosensitive polyimide Process," *MEMS* 92, p. 87, 1992.

Physical Sensors

9. Ko, W. H., and C. D. Fung, "VLSI and intelligent transducers," *Sensors and Actuators*, 2, pp. 239–250, 1982.
10. Lahiji, G. R., and K. D. Wise, "A monolithic thermopile detector fabricated using integrated-circuit technology," *Proc. Int. Electron. Dev. Meeting*, p. 676, 1980.
11. Ko, W. H., "Solid state capacitive pressure transducers," *Sensors and Actuators*, 10, pp. 303–320, 1986.
12. Ko, W. H., M. H. Bao, and Y. D. Hong, "A high sensitivity integrated circuit capacitive pressure transducer," *IEEE Trans. Elect. Dev*., ED-29, pp. 48–56, 1982.
13. Seitz, W. R., "Chemical sensors based on fiber optics," *Anal. Chem*., 56, 16A–34A, 1984.
14. Baltes, H. P., and R. S. Popovic, "Integrated semiconductor magnetic field sensors," *Proc. IEEE*, 74, pp. 1107–1132, 1986.

Chemical and Biomedical Sensors

15. Madou, M. J., and S. R. Morrison, "Chemical Sensing with Solid State Devices," Academic Press, 1989.
16. Microfabricated Systems and MEMS VI, Proceedings Vol. 2002–6, The Electrochemical Society, P. J. Hesketh et al. (ed.), 2002.
17. Schmitte, F. J., and G. Wiegleb, "Conductivity behavior of thick film Tin-dioxide gas sensors," *Sensors and Actuators*, 84, p. 473, 1991.
18. Torvela, H., A. Harkona-Mattila, and S. Leppavori, "Characterization of a combustion process using catalyzed Tin-oxide gas sensor to detect CO from emission gases," *Sensors and Actuators*. Bl, p. 83, 1990.
19. Gall, M., "The Si planar pellistor: a low-power pellistor sensor in Si thin film technology," *Sensors and Actuators*, B4, p. 533, 1991.
20. Accorsi, A., G. Delapierre, C. Vauchier, and D. Charlot, "A new microsensor for environmental measurements," *Sensors and Actuators*, B4, p. 539, 1991.

Downloaded from Digital Engineering Library @ McGraw-Hill (www.digitalengineeringlibrary.com)
Copyright © 2004 The McGraw-Hill Companies. All rights reserved.
Any use is subject to the Terms of Use as given at the website.

21. Hesketh, P. J., L. Smith, M. Gerber, T. Wulff, and J. Joseph, "Thermal stability of thin filmthermopile sensors," in Proc. 3rd Internat. Meeting on Chem. Sensors, p. 389, 1990.
22. Muehlbauer, M. J., E. J. Guilbeau, and B. C. Towe, "Model for a thermoelectric enzyme glucose sensor," *Anal. Chem.*, 61, p. 77, 1989.
23. Turner, A. F. P., I. Karube, and G. S. Wilson (eds.), "Biosensors: Fundamentals and Applications," Oxford Science Publications, 1987.
24. Blum, L. J., and P. R. Coulet (eds.), "Biosensor Principles and Applications," Marcel Dekker, 1991.
25. Turner, A. F. P. (ed.), "Advances in Biosensors: A Research Annual," JAI Press, 1991.

Microactuators

26. Fujita, H., and K. Gabriel, "New Opportunities for Microactuators," in Technical Digest, 6th International Conference Solid-State Sensors and Actuators, pp. 14–20, June 1991.
27. Feury, A. M., T. L. Poteat, and W. S. Trimmer, "A Micromachined Manipulator for Submicron Positioning of Optical Fibers," in Technical Digest, IEEE Solid-State Sensor Workshop, June 1986.
28. Moroney, R. M., R. M. White, and R. T. Howe, "Ultrasonic Micromotors: Physics and Applications," in Proceedings, IEEE Micro Electro Mechanical Systems Workshop, pp. 182–187, February 1990.
29. Guckel, H., T. R. Christenson, K. J. Skrobis, J. Klein, and M. Karnowsky, "Design and Testing of Planar Magnetic Micromotors Fabricated by Deep X-ray Lithography and Electroplating," in Technical Digest, 7th International Conference Solid-State Sensors and Actuators, pp. 60–64, June 1993.
30. Ahn, C., H. Y., J. Kim, and M. G. Allen, "A Planar Variable Reluctance Magnetic Micromotor with Fully Integrated Stator and Wrapped Coil," in Proceedings, IEEE Micro Electro Mechanical Systems Workshop, pp. 1–6, February 1993.
31. Wagner, B., M. Kreutzer, and W. Benecke, "Linear and Rotational Magnetic Micromotors Fabricated Using Silicon Technology," in Proceedings, IEEE Micro Electro Mechanical Systems Workshop, Travemunde, pp. 183–189, February 1992.
32. Guckel, H., K. J. Skrobis, T. R. Christenson, J. Klein, S. Han, B. Choi, E. G. Lovell, and T. W. Chapman, "Fabrication and testing of the planar magnetic micromotor," *J. Micromech. Microeng*. 1, pp. 135–138, September 1991.
33. Riethmuller, W., and W. Benecke, "Thermally excited silicon microactuators," *IEEE Trans. Electron Dev*., 35, p. 758, 1988.
34. Schetky, L. M., "Shape-memory alloy," *Scientific American*, 241, p. 74, Nov. 1979.
35. Walker, J. A., K. J. Gabriel, and M. Mehregany, "Thin-film processing of TiNi shape memory alloy," *Sensors and Actuators*, A21–A23, p. 243, 1990.
36. Johnson, A. D., "Vacuum deposited TiNi shape memory film: Characterization and application in microdevices," *J. Micromech. Microeng*. 1, p. 34, 1991.
37. Buehler, W. J., J. V. Gilfrich, and R. C. Wiley, "Effect of low-temperature phase changes on the mechanical properties of alloys near composition TiNi," *J. Appl. Phys*., 34, p. 1475, 1963.
38. Wang, F. E., and W. J. Buehler, "Additional unique property changes observed during TiNi transition," *Appl. Phys. Lett*., 21, p. 105, 1972.
39. Zdeblick, M. J., and J. B. Angell, "A Microminiature Electro-Fluidic Valve," in Technical Digest, 4th International Conference on Solid-State Sensors and Actuators, p. 827, June 1987.
40. Bart, S. F., T. A. Lober, R. T. Howe, J. H. Lang, and M. F. Schlecht, "Design considerations for micromachined electric actuators," *Sensors and Actuators*, 14, p. 269–292, July 1988.
41. Jennan, H., "Electrically-Activated, Normally-Closed Diaphragm Valves," in Technical Digest, 6th International Conference on Solid-State Sensors and Actuators, pp. 1045–1048, June 1991.
42. Busch, J. D., and A. D. Johnson "Prototype Micro-Valve Actuator," in Proceedings, IEEE Micro Electro Mechanical Systems Workshop, p. 40, February 1990.
43. Zengerle, R., A. Richter, and H. Sandmaier, "A Micro Membrane Pump with Electrostatic Actuation," in Proceedings, IEEE Micro Electro Mechanical Systems Workshop, pp. 19–24. February, 1992.
44. Tang, W. C., T. H. Nguyen, and R. T. Howe, "Laterally driven polysilicon resonant microstructures," *Sensors and Actuators*, 20, pp. 25–32, 1989.
45. Gianchandani, Y. B., and K. Najafi, "A bulk silicon wafer dissolved process for microelectromechanical devices," *J. Microelectromech. Syst.*, 1, pp. 77–85, June 1992.

Downloaded from Digital Engineering Library @ McGraw-Hill (www.digitalengineeringlibrary.com)
Copyright © 2004 The McGraw-Hill Companies. All rights reserved.
Any use is subject to the Terms of Use as given at the website.

MICROSENSORS AND MICROACTUATORS

46. Takeshima, N., K. Gabriel, M. Ozaki, J. Takahashi, H. Horiguchi, and H. Fujita, "Electrostatic Parallelogram Actuators," in Technical Digest, 6th International Conference on Solid-State Sensors and Actuators, pp. 63–66, June 1991.

47. Brennen, R. A., M. G. Lim, A. P. Pisano, and A. T. Chou, "Large Displacement Linear Actuator," in Technical Digest, IEEE Solid-State Sensors and Actuators Workshop, pp. 135–139, June 1990.

48. Deng, K., M. Mehregany, and A. S. Dewa, "A Simple Fabrication Process for Side-Drive Micromotors," in Technical Digest, 7th International Conference Solid-State Sensors and Actuators, pp. 756–759, June 1993.

49. Mehregany, M., and Y. C. Tai, "Surface micromachined mechanisms and micromotors," *J. Micromech. Microeng*. l, pp. 73–85, June 1992.

50. Omar, M. P., M. Mehregany, and R. L. Mullen, "Modeling of electric and fluid fields in silicon microactuators," *Int. J. Appl. Electromagnet. Mater*., 3, pp. 249–252, 1993.

51. Mehregany, M., "Microfabricated Silicon Electric Mechanisms," Ph.D. Thesis, Massachusetts Institute of Technology, June 1990.

52. Mehregany, M., S. F. Bart, L. S. Tavrow, J. H. Lang, S. D. Senturia, and M. F. Schlecht, "A study of three microfabricated variable-capacitance motors," *Sensors and Actuators*, A21–A23, pp. 73–179, February–April 1990.

53. Mehregany, M., S. F. Bart, L. S. Tavrow, J. H. Lang, and S. D. Senturia, "Principles in design and microfabrication of variable-capacitance side-drive motors," *J. Vac. Sci. Tech. A*, 8, pp. 3614–3624, July–August 1990.

54. Bart, S. F., M. Mehregany, L. S. Tavrow, J. H. Lang, and S. D. Senturia, "Electric micromotor dynamics," *IEEE Trans. Electron Dev.*, ED-39, pp. 566–575, March 1992.

55. Mehregany, M., S. D. Senturia, and J. H. Lang, "Measurement of wear in polysilicon micromotors," *IEEE Trans. Electron Dev.*, ED-39, pp. 1136–1143, May 1992.

56. Mehregany, M., S. D. Senturia, J. H. Lang, and P. Nagarkar, "Micromotor fabrication," *IEEE Trans. Electron Dev*. ED-39, pp. 2060–2069, September 1992.

57. Mehregay, M., and V. R. Dhuler "Operation of electrostatic micromotors in liquid environments," *J. Micromech. Microeng.*, 2, pp. 1–3, March 1992.

58. Dhuler, V. R., M. Mehregany, S. M. Phillips, and J. H. Lang, "A Comparative Study of Bearing Designs and Operational Environments for Harmonic Side-Drive Micromotors," Proceedings, IEEE Micro Electro Mechanical Systems Workshop. pp. 171–176, February 1992.

BIBLIOGRAPHY

A. Books

Gopel, W., J. Hesse, and J. N. Zemel (eds.), "Sensors—A Comprehensive Survey," VCH publisher, 1989.

Kovacs, G. T. A., "Micromachined Transducers—Sourcebook," McGraw-Hill, 1998.

Madou, M., "Fundamental of Microfabrication," 2nd ed., CRC Press, 2002.

Madou, M. J., and S. R. Morrison, "Chemical Sensing with Solid State Devices," Academic Press, 1989.

Maluf, N., "An Introduction to Microelectromechanical System Engineering," Artech House, 2000.

Norton, H. M., "Handbook of Transducers," Prentice Hall, 1989.

Senturia, S. D., "Microsystem Design," Kluwer Academic, 2001.

Sze, S. M. (ed.), "Semoconductor Sensors," Wiley, 1994.

Wolf, S., and R. N. Tauber, "Silicon Processing for the VLSI Era, Volume I—Process Technology," Lattice Press, 1986.

B. Journals

IEEE Transactions on Electron Devices. &. Special issues, ED-26 (1979), ED-29 (1982).

Journal of MEMS, IEEE and ASME (1992–present).

Journal of Micromechanics and Microengineering, Institute of Physics (1991–present).

Microsystems Technologies, Springer International, (1994–present).

Sensors and Actuators, Elsevier (1980–present) monthly, part A physical, part B chemical.

Sensors and Materials, MYU, (1989–present).

Downloaded from Digital Engineering Library @ McGraw-Hill (www.digitalengineeringlibrary.com)
Copyright © 2004 The McGraw-Hill Companies. All rights reserved.
Any use is subject to the Terms of Use as given at the website.

C. Conference Proceedings and Technical Digests

Asian Pacific Transducers and Micro/Nano Technologies Conference (2002).

Europe Sensors and Microsystems Conferences (1990, yearly).

IEEE/MEMS Workshop, IEEE (1987, 1989–2002, yearly).

International Meetings on Chemical Sensors (1983, 1986, 1990, 1992, 1994, 1996, 1998.).

Japan Sensor Symposia (annually 1981–2002, yearly).

Microfabricated Systems and MEMS VI, Proceedings Vol. 2002-4, The Electrochemical Society, P. J. Hesketh et al. (ed) (2002–2004, even years).

Sensors and Actuators Workshops (1986–2002, even years).

Sensor Expo in United States of America (1990–2002, yearly).

Transducer Conferences (1981–2001, odd years).

Downloaded from Digital Engineering Library @ McGraw-Hill (www.digitalengineeringlibrary.com)
Copyright © 2004 The McGraw-Hill Companies. All rights reserved.
Any use is subject to the Terms of Use as given at the website.